CANCER GENOMICS & PROTEOMICS *19*: 305-327 (2022)
doi:10.21873/cgp.20322

Prognostic Relevance of ZNF844 and Chr 19p13.2 KRAB-Zinc Finger Proteins in Clear Cell Renal Carcinoma

SIMONE O. HEYLIGER[1], KARAM F.A. SOLIMAN[2], MARILYN D. SAULSBURY[1] and R. RENEE REAMS[2]

[1]*Department of Pharmaceutical Sciences, Hampton University, Hampton, VA, U.S.A.;*
[2]*College of Pharmacy and Pharmaceutical Sciences, Florida A&M University, Tallahassee, FL, U.S.A.*

Abstract. *Background/Aim: Clear-cell renal cell carcinoma (ccRCC) is the most common and aggressive form of all urological cancers, with poor prognosis and high mortality. Despite growing evidence of involvement in carcinogenesis, the role of KRAB-ZFP in ccRCC has not been fully explored. KRAB Zinc finger proteins (KRAB-ZFPs) are the largest family of mammalian transcription regulators. They are differentially expressed in various tissues during cellular development and phenotypic differentiation. Materials and Methods: In this study, the levels of transcripts of ccRCC from The Cancer Genome Atlas (TCGA) dataset were used to identify prognostic biomarkers in this disease. Results: Using bioinformatics techniques, we demonstrate that approximately 60% of KRAB zinc finger proteins located on chromosome 19p13.2 are differentially expressed, with all but two being down-regulated in ccRCC. Moreover, ZNF844, a paralog of ZNF433, was the most down-regulated across all histological grades and pathological stages ($p<0.001$). In addition, the decrease in ZNF844 expression was associated with poor patient survival (HR=0.41; 95% CI=0.3-0.56; $p<0.0001$). Gene Set Enrichment Analysis of genes inversely co-expressed with ZNF844 revealed that enriched pathways were consistently related to immune and translation processes ($p<0.05$, FDR <0.05). Lastly, ZNF844 expression showed moderate, inverse correlation to Helper T-cell (CD4 or Th1) subtype 1 ($R=–0.558$, $p=5.15\times10^{-39}$) infiltration and with the exhausted T-cell phenotype ($R=–0.37$; $p=4.1\times10^{-21}$). Conclusion: Down-regulation of KRAB-ZFPs at 19p13.2 may represent a signature for ccRCC. Moreover, ZNF844 is a prognostic marker for ccRCC and may serve as a putative immune-related tumor suppressor gene.*

Correspondence to: R. Renee Reams, Ph.D., College of Pharmacy and Pharmaceutical Sciences, Florida A&M University, 1415 South MLK Blvd, Tallahassee, FL 32307, U.S.A. Tel: +1 8505612672, e-mail: renee.reams@famu.edu

Key Words: ZNF844, ZNF433, clear cell renal carcinoma, Kruppel-associated box, KRAB-ZFPs, tumor microenvironment, ccRCC, Th1 cells, biomarker, Chr19p13.2.

This article is an open access article distributed under the terms and conditions of the Creative Commons Attribution (CC BY-NC-ND) 4.0 international license (https://creativecommons.org/licenses/by-nc-nd/4.0).

Clear cell renal carcinoma (ccRCC) is the most common neoplastic disease affecting the kidneys. It accounts for at least 70% of all kidney cancers (1, 2). In advanced stages, ccRCC becomes resistant to conventional therapies (1-3). Moreover, later stages are associated with poor prognosis with a 5-year overall survival rate of less than 10% (1-3). Despite growing evidence of involvement in carcinogenesis, the role of KRAB-ZFP in ccRCC has not been fully explored. Kruppel-associated box domain-containing zinc-finger proteins (KRAB-ZFP) represent the most prominent family of transcriptional repressors (4, 5). The human genome contains over 300 KRAB-ZFPs genes that produce more than 800 transcripts that encode proteins, pseudogenes, and splice variants (6-8). KRAB-ZFPs are differentially expressed in various tissues during cellular development. Several of these genes are involved in embryogenesis, genome imprinting, and biological processes that determine phenotypes in stem cells (9-11). Given their roles in cellular differentiation and their ability to alter gene expression *via* epigenetic processes and chromatin remodeling, it is conceivable that dysregulation of KRAB-ZFP transcription factors could facilitate tumorigenesis and tumor progression.

Interestingly, several large KRAB-ZFP clusters are located on chromosome 19 (chr19), and several studies have linked genetic alterations in chromosome 19p13 to cancers (12-18). Using data mining techniques, we recently identified ZNF433, a zinc finger that is differentially expressed in ccRCC (19) and that may be a biomarker for ccRCC. ZNF433 is part of a cluster of KRAB-ZFPs that are located on chromosome 19p13.2. Thus, we focused on this locus to ascertain if the expression of other members of this cluster was altered. We have identified several KRAB-ZFPs that are differentially expressed and are associated with changes in overall survival in patients. Since the gene ZNF844 is a paralog of ZNF433, it appears to be a strong candidate biomarker and prognostic factor for ccRCC.

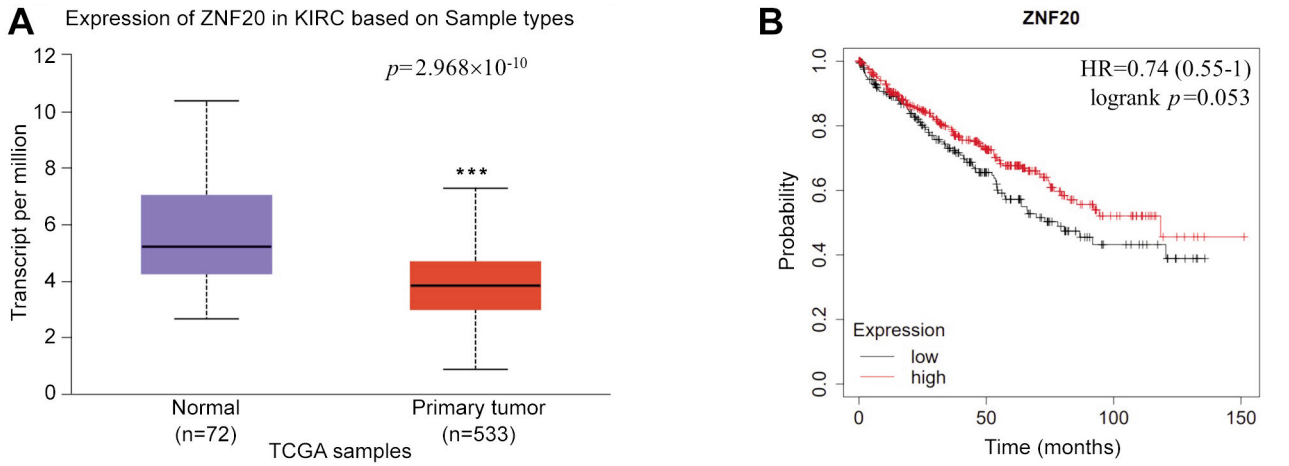

Figure 1. *Differential expression of KRAB zinc finger protein 20 (ZNF20). A: mRNA expression of ZNF20 in normal and clear cell renal carcinoma tumors. B: Kaplan-Meier survival plot for ZNF20 high expression and low expression groups. K-M plot was generated using the KM plotter web tool. *** denotes p<0.001.*

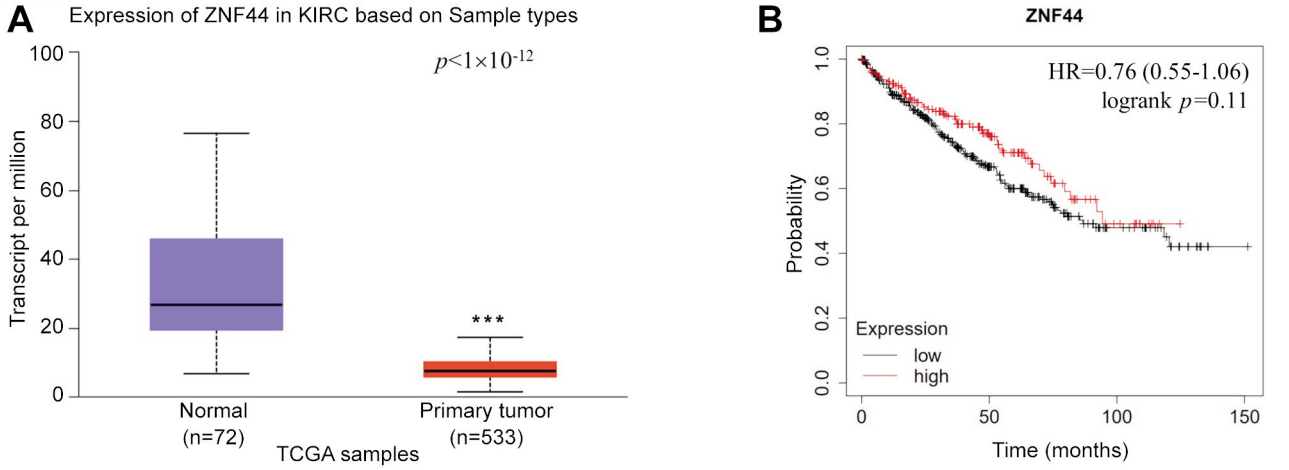

Figure 2. *Differential expression of KRAB zinc finger protein 44 (ZNF44). A: mRNA expression of ZNF44 in normal and clear cell renal carcinoma tumors. B: Kaplan-Meier survival plot for ZNF44 high expression and low expression groups. K-M plot was generated using the KM plotter web tool. *** denotes p<0.001.*

Materials and Methods

UALCAN (gene expression) analysis. In this study, UALCAN (http://ualcan.path.uab.edu/analysis.html) (accessed on June 5, 2021 and on August 25, 2021) was used to ascertain whether chromosome 19p13.2 KRAB-ZFPs were differentially expressed in ccRCC. UALCAN is an online open-access web tool that provides graphical visualizations of pathological clinic features, gene expression data, promoter methylation data derived from TCGA KIRC RNA-Seq data, as well as protein expression data derived from the CPTAC dataset (20). UALCAN was used to examine the mRNA expression of ZNF844 in relationship to clinicopathological parameters (cancer stage and grade) of ccRCC. To illustrate gene expression data in graphs, gene symbols for various KRAB-ZFPs were inputted into the 'scan by gene' query box, and the kidney renal clear cell carcinoma (KIRC) was selected. Graphical representations of gene expression data as a function of clinicopathological and demographic data were obtained by selecting the search feature on the website.

UCSC Xena and GEO databases (gene expression validation). To validate gene expression results obtained from UALCAN, TCGA KIRC clinical information, and RNA sequencing dataset (*n*=538) were downloaded from the UCSC XENA portal (https://xena.ucsc.edu/public/) (21) on July 27, 2021. To obtain the data, the KIRC-TCGA study was selected. Under the querying system, genomic data of KRAB ZFP of interest was chosen as the first variable. For the second variable, phenotypic data for the sample type, age at initial pathologic diagnosis, sex, pathologic N, pathologic stage, neoplastic histological grade, and genomic information for ID TCGA-HiSeqV2 data were selected. Primary tumors were selected as a filter

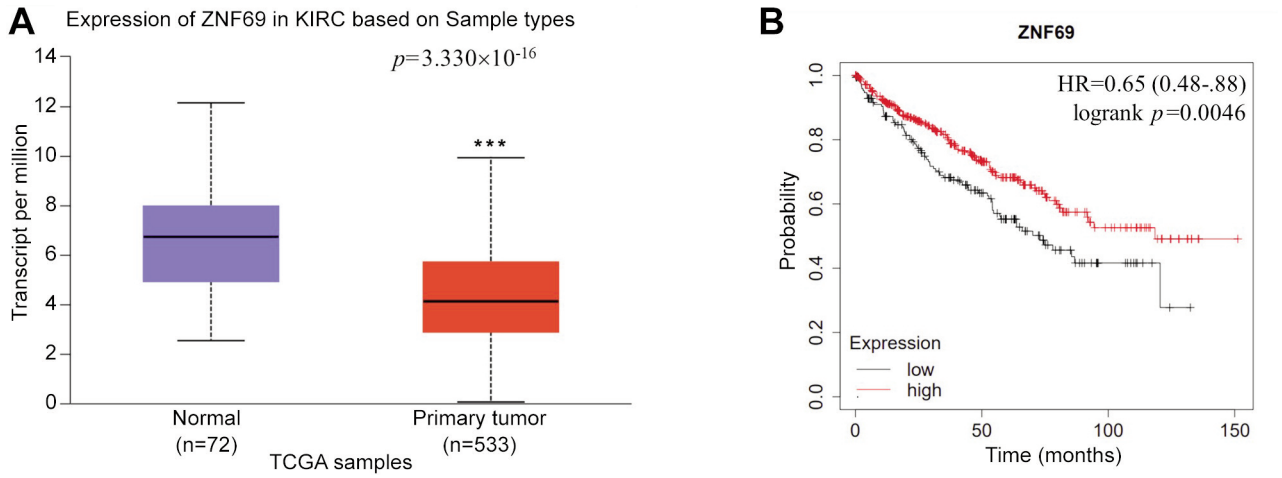

Figure 3. *Differential expression of KRAB zinc finger protein 69 (ZNF69). A: mRNA expression of ZNF69 in normal and clear cell renal carcinoma tumors. B: Kaplan-Meier survival plot for ZNF69 high expression and low expression groups. K-M plot was generated using the KM plotter web tool. *** denotes p<0.001.*

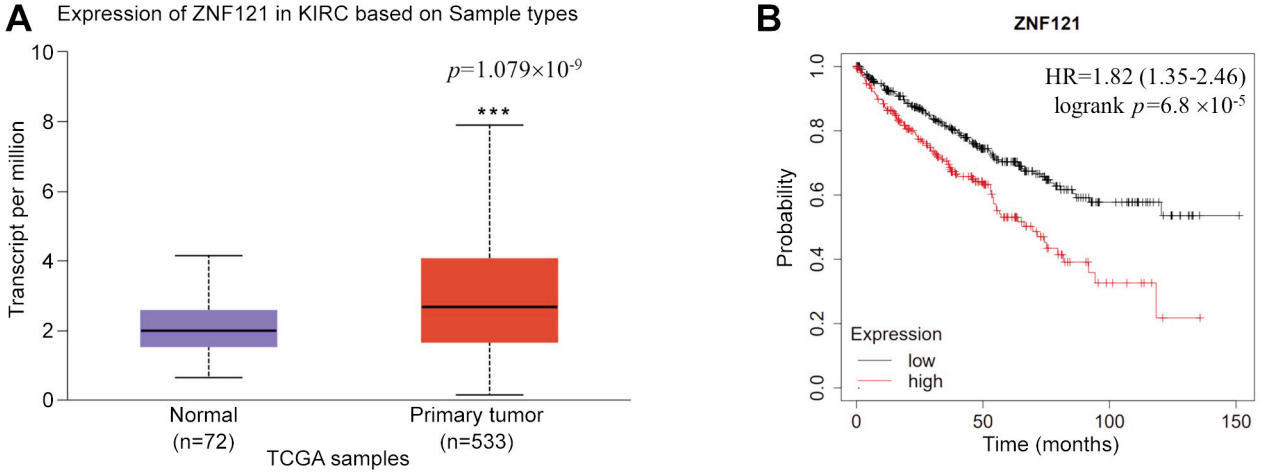

Figure 4. *Differential expression of KRAB zinc finger protein 121 (ZNF121). A: mRNA expression of ZNF121 in normal and clear cell renal carcinoma tumors. B: Kaplan-Meier survival plot for ZNF121 high expression and low expression groups. K-M plot was generated using the KM plotter web tool. *** denotes p<0.001.*

to remove duplications in the data, leaving 538 samples. To ascertain survival data, KM analysis feature was selected under the first variable results, and the raw data was downloaded. Data was utilized to generate Kaplan-Meier plot to ascertain the impact of gene expression on patient survival. Moreover, data was also used to perform ROC/AUC analysis as well as univariate and multivariate analyses to ascertain whether ZNF844 and other KRAB-ZFPs were predictive ccRCC biomarkers. In addition, we also downloaded patient data (GSE12606) from Gene Expression Omnibus GEO (http://www.ncbi.nlm.nih.gov/geo/) database (22). GEO2R was used to analyze ZNF844 gene expression between normal and metastatic ccRCC. The adjusted *p*-Value significance was set at 0.05.

GEPIA database analysis (gene expression and correlation analysis). GEPIA2 database is an enhanced version of GEPIA. This gene expression database includes gene and corresponding isoforms in normal and tumor samples of 84 cancer subtypes derived from The Cancer Genome Atlas (TCGA) and Genotype-Tissue Expression (GTEx) databases (23-25). GEPIA2 was used to conduct correlation analysis between ZNF844 expression and T-cell signatures. GEPIA2 was accessed on December 12, 2021 (http://gepia2.cancer-pku.cn). To perform this function, the "Correlation Analysis" module was chosen, and ZNF844 for was entered into the Gene A query box, and the desired T-cell signature was chosen. These included naïve T-cell signature (*genes: CCR7, LEF1, TCF7, SELL*), Helper T-cell Type 1 signature (*genes: CXCL13, HAVCR2, IFNG, CXCR3, CD4, BHLHE40*), Helper T-cell Type 2 signature (*genes: CCL26, IL5, IL13, GATA3, STAT6*), Effector T-reg signature (*genes: FOXP3, CTLA4, CCR8, TNFRSF9*), Effector T-cell signature (*genes: CX3CR1, FGFBP2, FCGR3A*), and the Exhausted T-cell signature (*genes: HAVCR2, TIGIT, LAG3, PDCD1,*

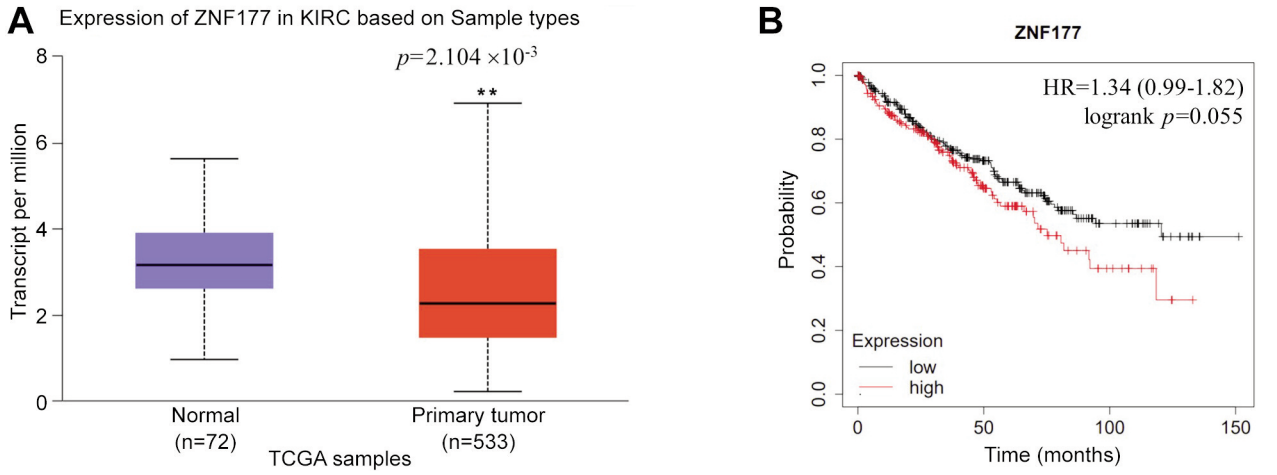

Figure 5. *Differential expression of KRAB zinc finger protein 177 (ZNF177). A: mRNA expression of ZNF177 in normal and clear cell renal carcinoma tumors. B: Kaplan-Meier survival plot for ZNF177 high expression and low expression groups. K-M plot was generated using the KM plotter web tool. ** denotes p<0.01.*

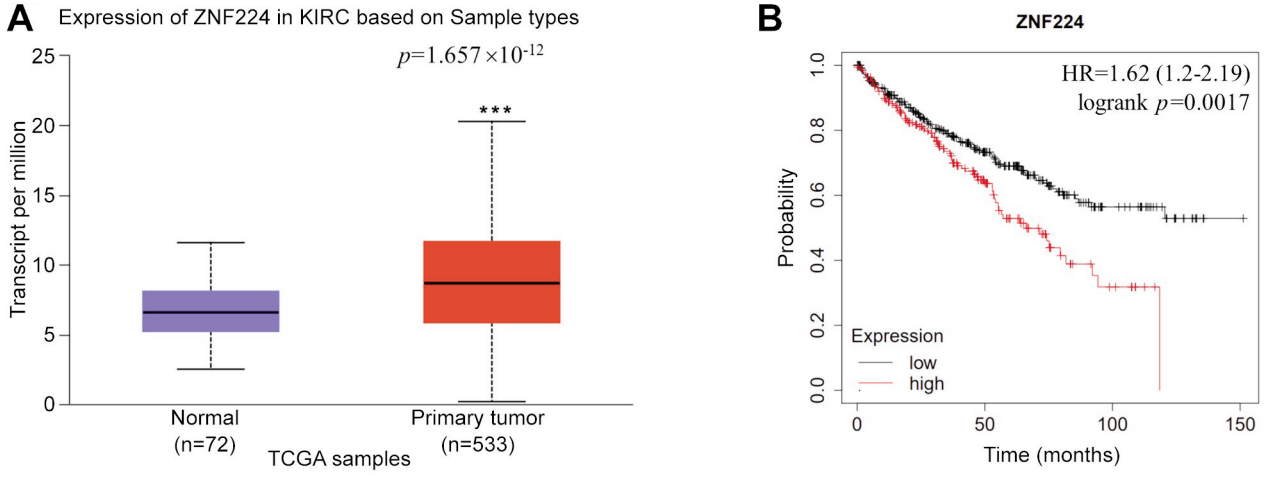

Figure 6. *Differential expression of KRAB zinc finger protein 224 (ZNF224). A: mRNA expression of ZNF224 in normal and clear cell renal carcinoma tumors. B: Kaplan-Meier survival plot for ZNF224 high expression and low expression groups. K-M plot was generated using the KM plotter web tool. *** denotes p<0.001.*

CXCL13, LAYN). To analyze the correlation between ZNF844 and various aforementioned gene signatures, Pearson correlation coefficient was utilized. *p*-Value significance was set at 0.05.

Human Protein Atlas Database (immunohistochemistry). Human Protein Atlas (HPA) was used to ascertain if the ZNF844 protein was differentially expressed in normal kidney and renal carcinomas (HPA, https://www.proteinatlas.org/) (accessed on June 5, 2021) (26). HPA provides qualitative analysis of the protein expression relative to normal tissues. In addition, HPA RNA-seq data were used to identify single cell types and gene clusters associated with expression of ZNF844 (accessed on February 2, 2022).

Timer 2.0. Database (tumor microenvironment). TIMER2.0 (http://timer.cistrome.org/) (accessed on June 26, 2021) was used to examine ZNF844 expression *versus* immune infiltration using the XCell algorithm. The TIMER 2.0 web tool provides a robust estimation of immune infiltration levels for The Cancer Genome Atlas (TCGA) or user-provided tumor profiles using six state-of-the-art algorithms (27, 28). In addition, TIMER2.0 provides modules for investigating the associations between immune infiltrates and genetic or clinical features, clinical outcomes and for exploring cancer-related associations in the TCGA cohorts (27, 28). All TCGA tumor data, including transcriptome profiles, somatic mutation calls, somatic copy number variations, and patient clinical outcomes, are collected from the GDAC firehose website (27, 28).

Linkedomics webtool (gene set enrichment analysis). The gene ontology (GO) enrichment analysis results of the genes co-expressed with ZNF844 were visualized using LinkedOmics

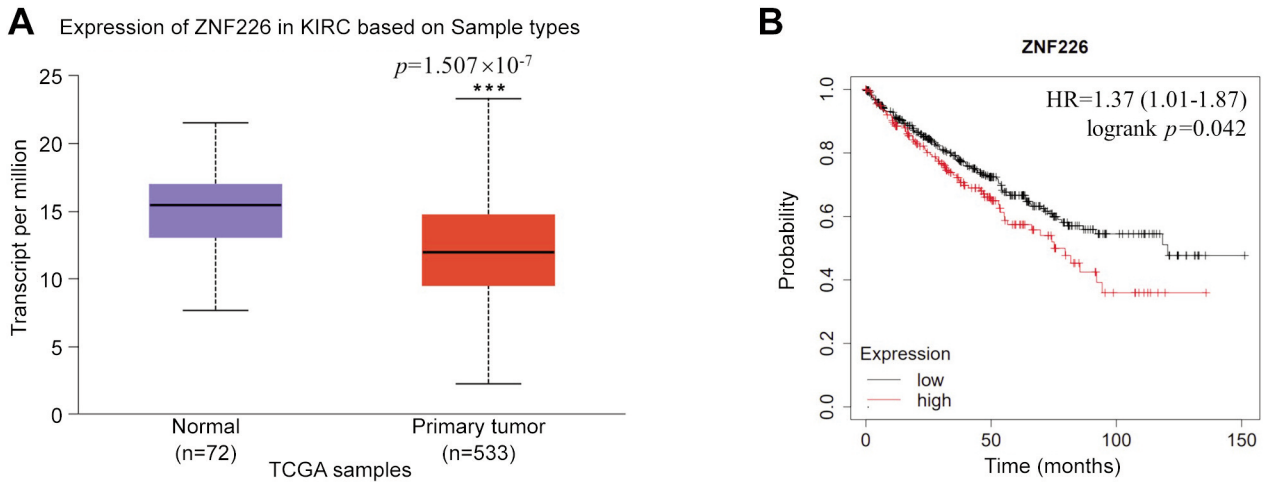

Figure 7. *Differential expression of KRAB zinc finger protein 226 (ZNF226). A: mRNA expression of ZNF226 in normal and clear cell renal carcinoma tumors. B: Kaplan-Meier survival plot for ZNF226 high expression and low expression groups. K-M plot was generated using the KM plotter web tool. *** denotes p<0.001.*

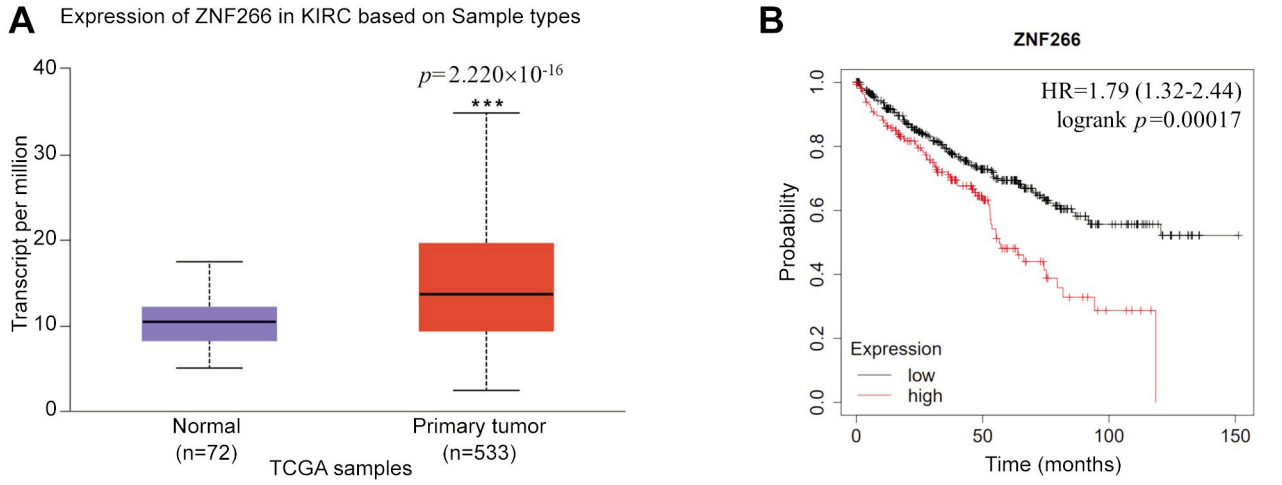

Figure 8. *Differential expression of KRAB zinc finger protein 266 (ZNF266). A: mRNA expression of ZNF266 in normal and clear cell renal carcinoma tumors. B: Kaplan-Meier survival plot for ZNF266 high expression and low expression groups. K-M plot was generated using the KM plotter web tool. *** denotes p<0.001.*

(http://www.linkedomics.org) (accessed on July 10, 2021). The LinkedOmics database contains multi-omics data and clinical data for 32 cancer types comprising 11,158 patients from the TCGA project (28). The "LinkFinder" module was used to visualize the differentially expressed genes within the TCGA KIRC cohort. The "LinkInterpreter" module was used to perform GSEA and ORA enrichment analysis methods to identify pathways that are enriched among genes positively and inversely expressed with ZNF844 within the GO Biological Process KEGG and Reactome databases. Results were analyzed for significance using the Pearson's correlation test with the *p*-value, and false discovery rate (FDR) set at 0.05.

Statistical analysis. For comparison gene expression in normal *versus* tumor samples, between male *versus* female between low grade and high-grade tumors, or between low and high-grade tumors, the Student *t*-test was used. Comparisons of ZNF844 gene expression across tumor stages and grades were conducted using one-way ANOVA with Tukey-Kramer post hoc analysis. Analysis of gene expression between the low histological grades or pathological stages *versus* higher grades and stages was conducted using the Student *t*-test. For the Kaplan-Meier (KM) survival outcome plots, Cox risk hazard ratio (HR), 95% confidence intervals (CI), and log-rank *p*-Values were generated by the KM plotter web tool. Receiver Operator Curve (ROC) analysis was performed to validate KM results using MedCalc statistical software and TCGA datasets downloaded *via* UCSC Xena webtool. An AUC greater than 0.6 is considered to mean that the gene has potential as a prognostic factor. The *p*-Value for all statistical sets was set at $p<0.05$ to indicate a statistical significance.

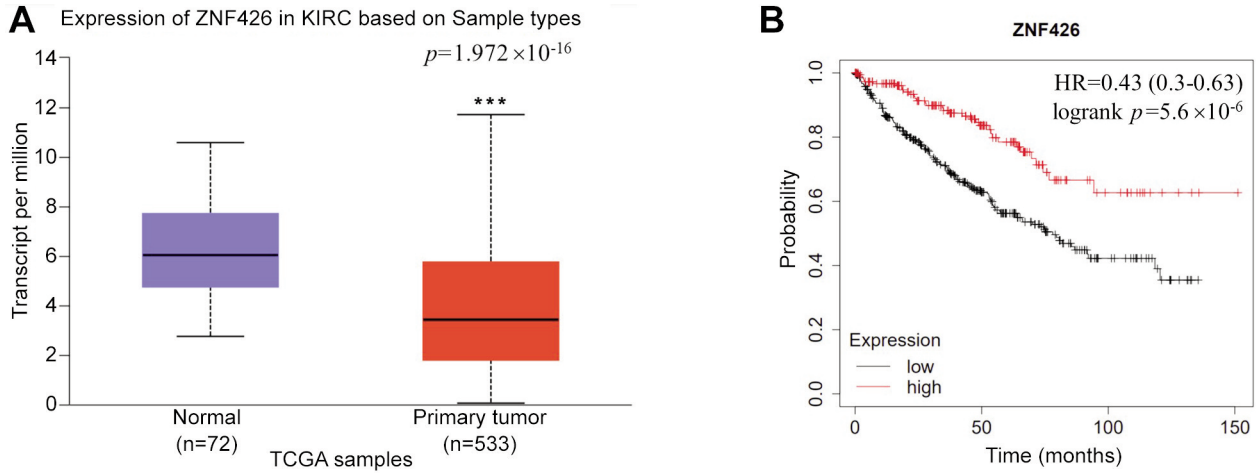

Figure 9. *Differential expression of KRAB zinc finger protein 426 (ZNF426). A: mRNA expression of ZNF426 in normal and clear cell renal carcinoma tumors. B: Kaplan-Meier survival plot for ZNF426 high expression and low expression groups. K-M plot was generated using the KM plotter web tool. *** denotes p<0.001.*

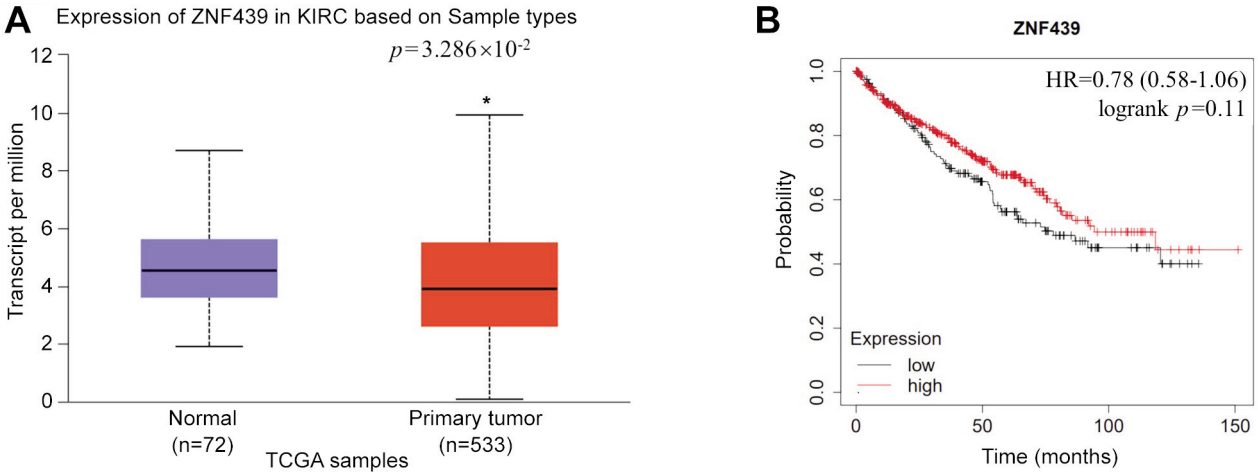

Figure 10. *Differential expression of KRAB zinc finger protein 439 (ZNF439). A: mRNA expression of ZNF439 in normal and clear cell renal carcinoma tumors. B: Kaplan-Meier survival plot for ZNF439 high expression and low expression groups. K-M plot was generated using the KM plotter web tool. * denotes the statistical significance of p<0.05.*

Results

Differential expression of KRAB-ZFPs at Chromosome 19p13.2. We analyzed 20 members of a cluster of KRAB-ZFPs located at the chromosome 19p13.2 locus. All (Figure 1, Figure 2, Figure 3, Figure 4, Figure 5, Figure 6, Figure 7, Figure 8, Figure 9, Figure 10, Figure 11, Figure 12, Figure 13, Figure 14, Figure 15, Figure 17, Figure 18, Figure 19 and Figure 20) but one, ZNF562 (Figure 16), were differentially expressed. Four KRAB-ZFP transcripts [ZNF121 (Figure 4A), ZNF224 (Figure 6A), ZNF 266 (Figure 8A), and ZNF700 (Figure 18A)] were up-regulated in ccRCC and were associated with unfavorable survival outcomes. Out of the fifteen KRAB-ZFPs that were down-regulated (Figure 1A, Figure 2A, Figure 3A, Figure 5A, Figure 7A, Figure 9A, Figure 10A, Figure 11A, Figure 12A, Figure 13A, Figure 14A, Figure 15A, Figure 17A, Figure 19A and Figure 20A), ten proteins [ZNF69 (Figure 3B), ZNF426 (Figure 9B), ZNF440 (Figure 11B), ZNF441 (Figure 12B), ZNF442 (Figure 13B), ZNF443 (Figure 14B), ZNF561 (Figure 15B), ZNF564 (Figure 17B), ZNF709 (Figure 19B) and ZNF844 (Figure 20B)] were associated with significant favorable survival outcomes ($p<0.05$). Analysis of the chr19p13.2 KRAB-ZFPs revealed that ZNF844 had the most significant changes in both

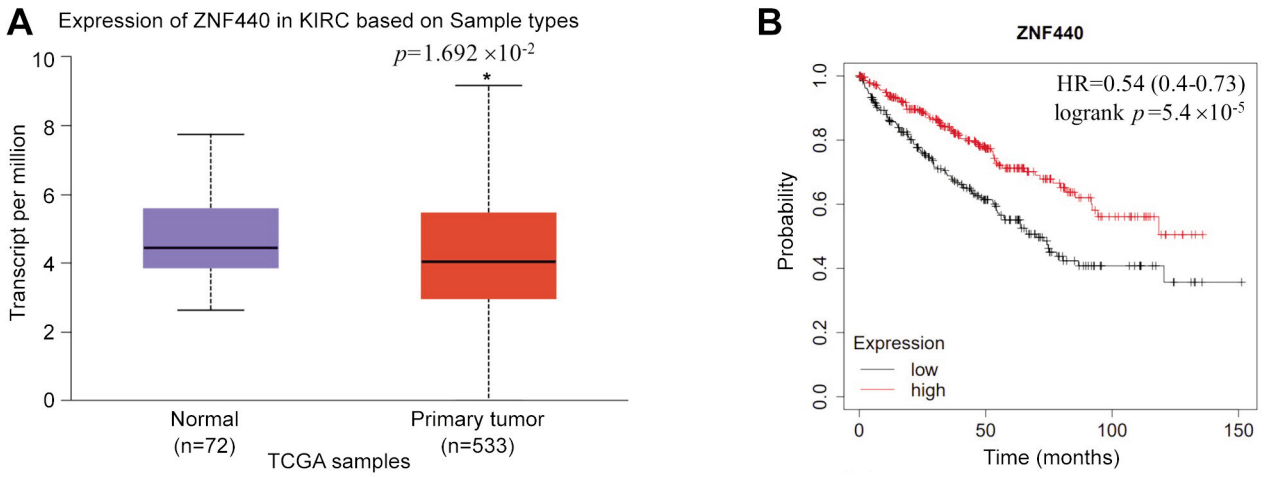

Figure 11. *Differential expression of KRAB zinc finger protein 440 (ZNF440). A: mRNA expression of ZNF440 in normal and clear cell renal carcinoma tumors. B: Kaplan-Meier survival plot for ZNF440 high expression and low expression groups. K-M plot was generated using the KM plotter web tool. *denotes the statistical significance of p<0.05.*

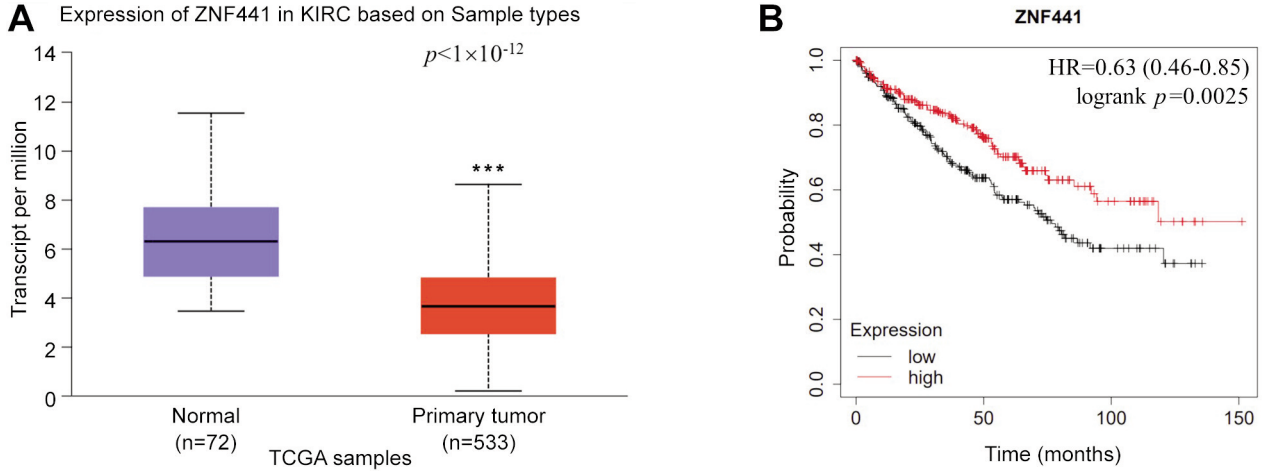

Figure 12. *Differential expression of KRAB zinc finger protein 441 (ZNF441). A: mRNA expression of ZNF441 in normal and clear cell renal carcinoma tumors. B: Kaplan-Meier survival plot for ZNF441 high expression and low expression groups. K-M plot was generated using the KM plotter web tool. *** denotes the statistical significance of p<0.001.*

gene expression (p=1.624×10^{-12}) and overall survival (p=9.4×10^{-8}), suggesting that this transcription factor may be a possible biomarker and prognostic indicator (Figure 20). Indeed, survival outcomes for the low expression group (less than 7.512 transcripts/million) were significantly lower than the high expression group (greater than 7.512 transcripts/million). To ascertain whether ZNF844 expression could discriminate between high-expression and low-expression groups in relationship to survival outcome, we conducted ROC analysis. The AUC was 0.642, 95% CI=0.599 to 0.683, indicating that ZNF844 expression is a moderate predictor of survival outcomes. Therefore, we further analyzed ZNF844 relative to clinicopathological features of ccRCC.

ZNF844 gene and protein expression in patients with clear-cell renal cell carcinoma. Figure 21 depicts the expression of ZNF844 protein in clear cell renal carcinoma and normal tissues. We utilized Human Protein Atlas (https://www.proteinatlas.org/) to identify immunohistochemistry images representing human normal and renal carcinoma tissues stained with antibodies raised against the ZNF844 protein (Figure 21A). The renal carcinoma images showed qualitatively that there was lower ZNF844 protein expression, as documented by descriptions that accompanied each image. Tissues from renal adenocarcinoma had "low" or "not detected" staining with "weak" intensities, whereas all normal tissues were described as having "medium" staining with "moderate" intensities. This suggests that these

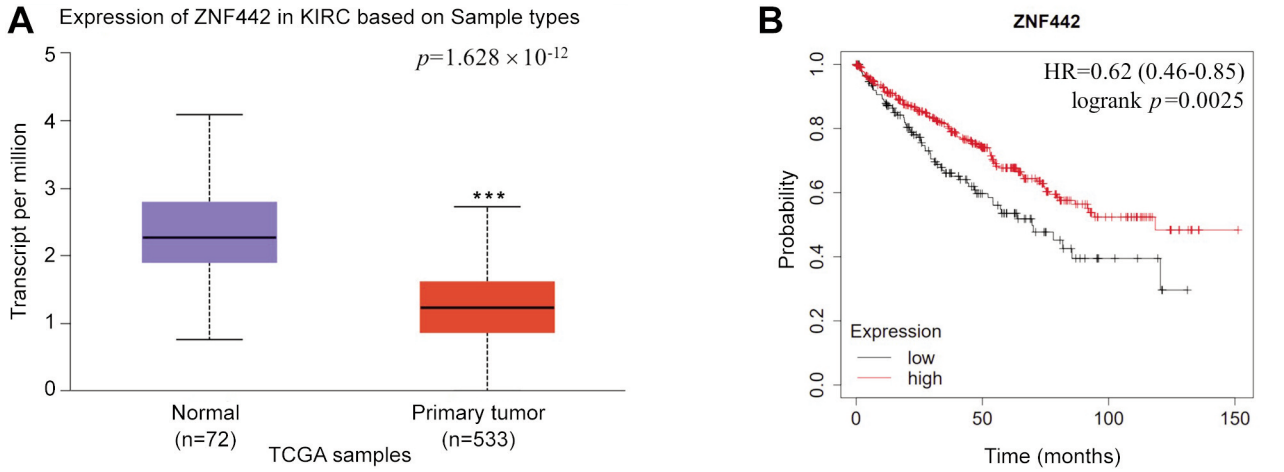

Figure 13. *Differential expression of KRAB zinc finger protein 442 (ZNF442). A: mRNA expression of ZNF442 in normal and clear cell renal carcinoma tumors. B: Kaplan-Meier survival plot for ZNF442 high expression and low expression groups. K-M plot was generated using the KM plotter web tool. *** denotes the statistical significance of p<0.001.*

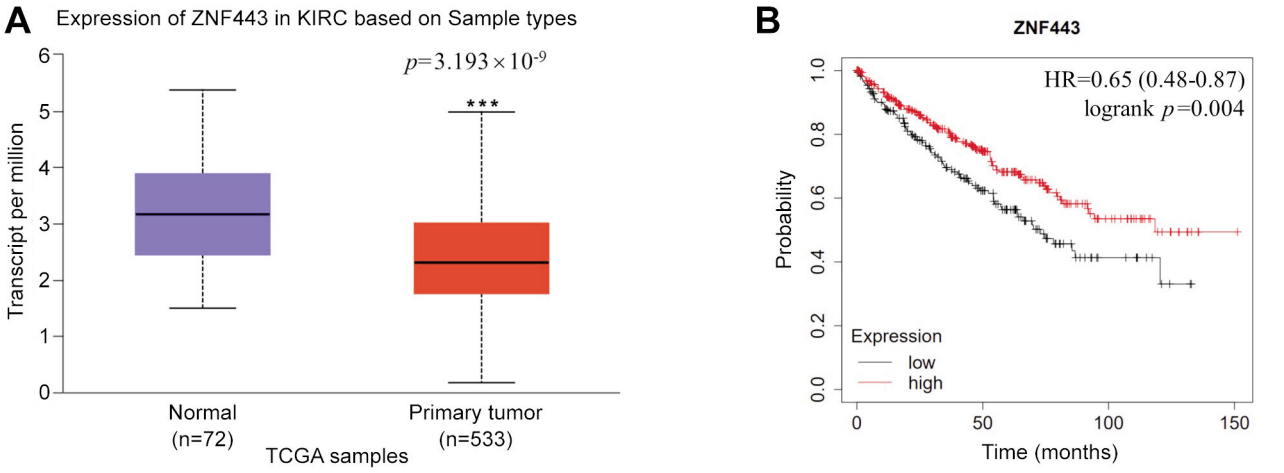

Figure 14. *Differential expression of KRAB zinc finger protein 443 (ZNF443). A: mRNA expression of ZNF443 in normal and clear cell renal carcinoma tumors. B: Kaplan-Meier survival plot for ZNF443 high expression and low expression groups. K-M plot was generated using the KM plotter web tool. ***denotes the statistical significance of p<0.001.*

representative, qualitative immunohistochemical images are consistent with reductions in transcript expression observed in Figure 20A. In addition, single cell map of the kidney (Figure 21B) revealed that ZNF844 expression within the kidney is associated with the cells proximal convoluted tubules and immune cells (macrophages, B-cells and T-cells). Lastly, analysis (Figure 21C) of expression data derived from metastatic and normal tissues (GSE12606) corroborated our TCGA-KIRC data by demonstrating that ZNF844 is significantly down-regulated (adjusted *p*-Value=0.025928).

ZNF844 gene expression in relationship to clinicopathological features. Table I provides the types of clinicopathological features, the corresponding numbers of each phenotype that were contained in the TCGA KIRC dataset. We further explored ZNF844 in relationship to age, pathological stage, histological grades, and nodal involvement. ZNF844 expression was significantly altered ($p<0.001$) across stages, grades, and nodal involvement but was not associated with sex ($p=0.838$) or age ($p=0.442$) (Table I).

To further characterize ZNF844, we examined the relationship between ZNF844 different clinicopathological features of clear cell renal carcinoma and survival outcome; we conducted multivariate and univariate Cox regression analysis (Table II). In the univariate model, age, stage, grade, and ZNF844 expression were predictive of survival outcome.

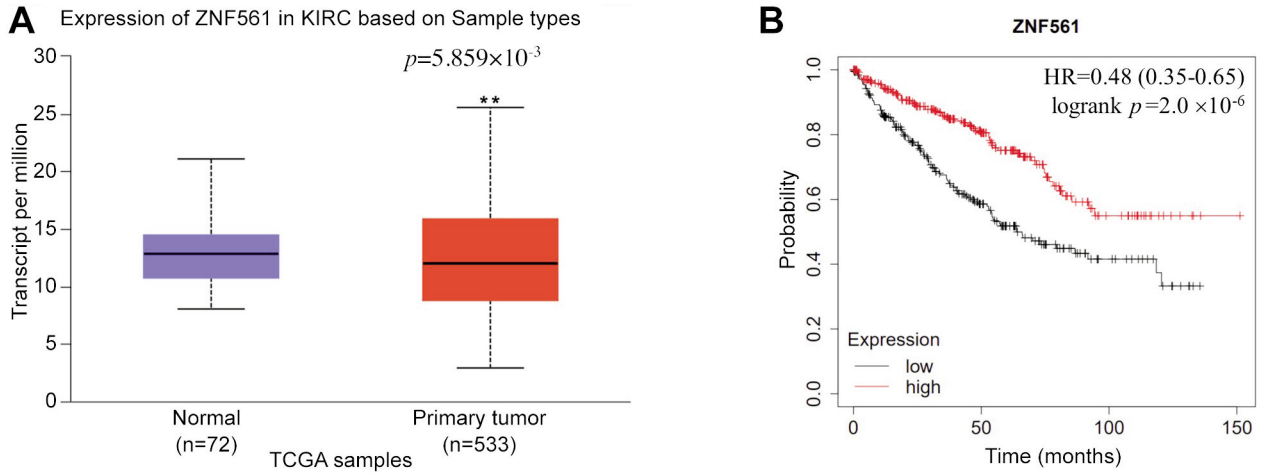

Figure 15. *Differential expression of KRAB zinc finger protein 561 (ZNF561). A: mRNA expression of ZNF561 in normal and clear cell renal carcinoma tumors. B: Kaplan-Meier survival plot for ZNF561 high expression and low expression groups. K-M plot was generated using the KM plotter web tool. **denotes the statistical significance of p<0.01.*

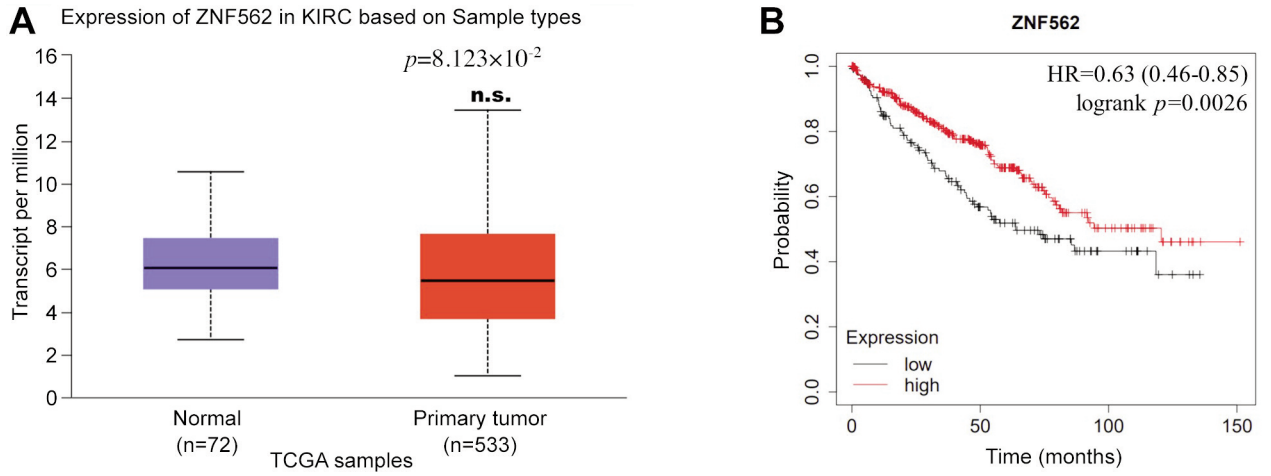

Figure 16. *Differential expression of KRAB zinc finger protein 562 (ZNF562). A: mRNA expression of ZNF562 in normal and clear cell renal carcinoma tumors. B: Kaplan-Meier survival plot for ZNF562 high expression and low expression groups. K-M plot was generated using the KM plotter web tool. "n.s." denotes that there was no statistical significance.*

In the multivariate model, age, stage, and ZNF844 expression retained predictive status, thereby indicating that ZNF844 may be a predictive biomarker for ccRCC.

In terms of ZNF844 expression across stages, ZNF844 transcripts were significantly lower ($p<0.001$) in all tumor stages relative to normal tissues (Figure 22A). Moreover, ZNF844 was differentially expressed across tumor stages [$F(4, 596)=186.314$, $df=4$, $p<0.001$], with the more advanced stages (3 and 4) having a lower expression of transcripts relative to stages 1 and 2 (Figure 22B). A similar pattern was also noted with regards to histological grades whereby ZNF844 expression was significantly down-regulated across all grades relative to normal tissues [$F(4, 571)=216.528$, $df=4$, $p<0.001$] (Figure 22C) and was significantly lower ($p<0.05$) in grades (3 and 4) relative to normal, grades 1 and 2 (Figure 22D).

ZNF844 pathway enrichment and gene ontology. Since there is limited information regarding ZNF844 target genes, we examined whether genes (Figure 23A-B) co-expressed with ZNF844 were components of overrepresented pathways. Specifically, we used Gene Set Enrichment Analysis (GSEA) to analyze KEGG,GO Biological Process and Reactome databases to identify enriched pathways (Figure 23C-E). Figure 23C provides the GSEA analysis of the genes co-

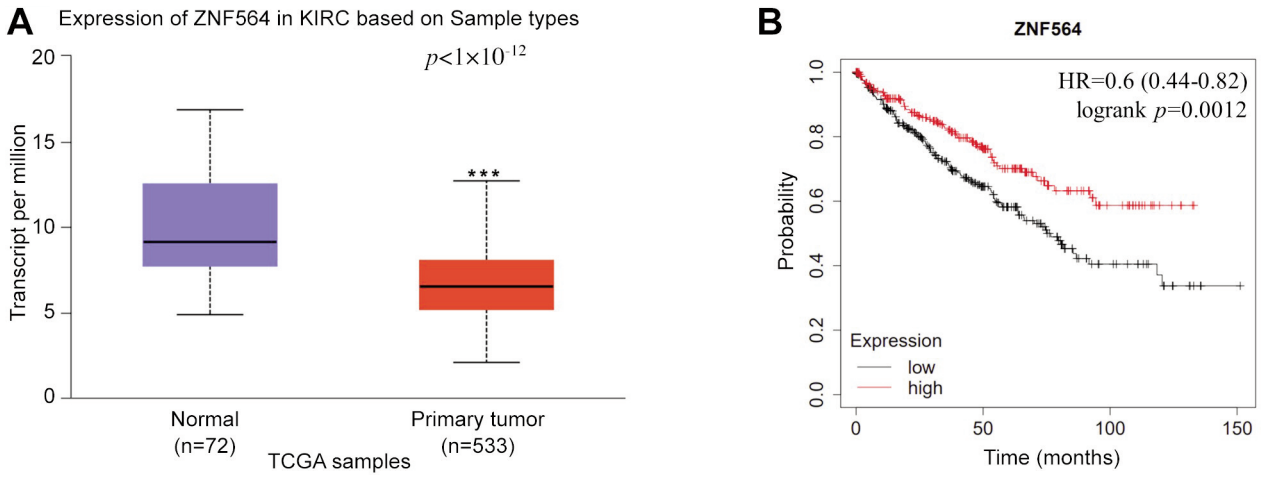

Figure 17. *Differential expression of KRAB zinc finger protein 564 (ZNF564). A: mRNA expression of ZNF564 in normal and clear cell renal carcinoma tumors. B: Kaplan-Meier survival plot for ZNF564 high expression and low expression groups. K-M plot was generated using the KM plotter web tool. *** denotes the statistical significance of p<0.001.*

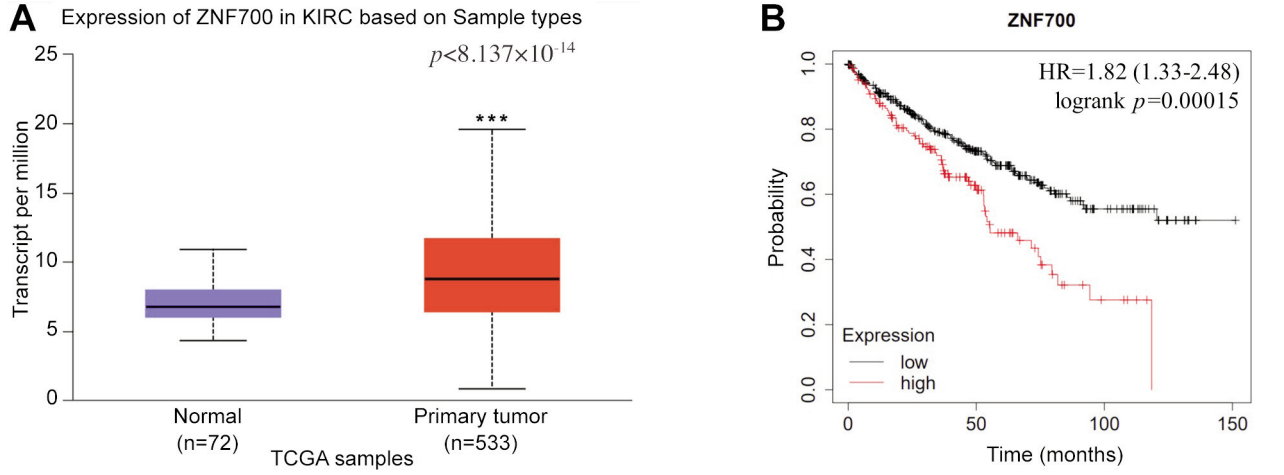

Figure 18. *Differential expression of KRAB zinc finger protein 700 (ZNF700). A: mRNA expression of ZNF700 in normal and clear cell renal carcinoma tumors. B: Kaplan-Meier survival plot for ZNF700 high expression and low expression groups. K-M plot was generated using the KM plotter web tool. *** denotes the statistical significance of p<0.001.*

expressed with ZNF844 using the GO biological processes (GOBP) database. For GSEA GOBP analysis, the most significantly enriched pathways [$p<0.05$; FDR (q value)<0.05] were found to be associated with inversely correlated genes. The top three enriched pathways were related to immune and translation processes. Immune-related pathways included humoral immune response (GO:0006959, 0.0091878, $p<1\times10^{-20}$, NES=–1.8716), response to interferon-gamma (GO:0034341 FDR=0.040801, $p<1\times10^{-20}$, NES=–1.6651), and adaptive immune response (GO:0002250, FDR=0.048321, $p<1\times10^{-20}$, NES=–1.6470). GSEA analysis of the KEGG database (Figure 23D) also revealed that immune-related and translation/transcription pathways were among the most significantly enriched pathways among inversely correlated genes ($p<0.05$; FDR<0.05). Immune-related pathways included Epstein-Barr virus infection (hsa05169), Cytokine-cytokine receptor interaction (hsa04060; $p<1\times10^{-20}$, FDR=0.012899, NES=–1.7121), Systemic lupus erythematosus (hsa05322; $p<1\times10^{-20}$, FDR=0.0024186, NES=–1.9218) and Pathogenic Escherichia coli infection (hsa05130; $p=<1\times10^{-20}$, FDR=0.016744, NES=–1.6932). Similar to the GOBP and KEGG databases, GSEA analysis of the Reactome database (Figure 23E) revealed the three most significantly enriched pathways among genes inversely expressed with ZNF844 were also related to transcription and antigen presentation (immune

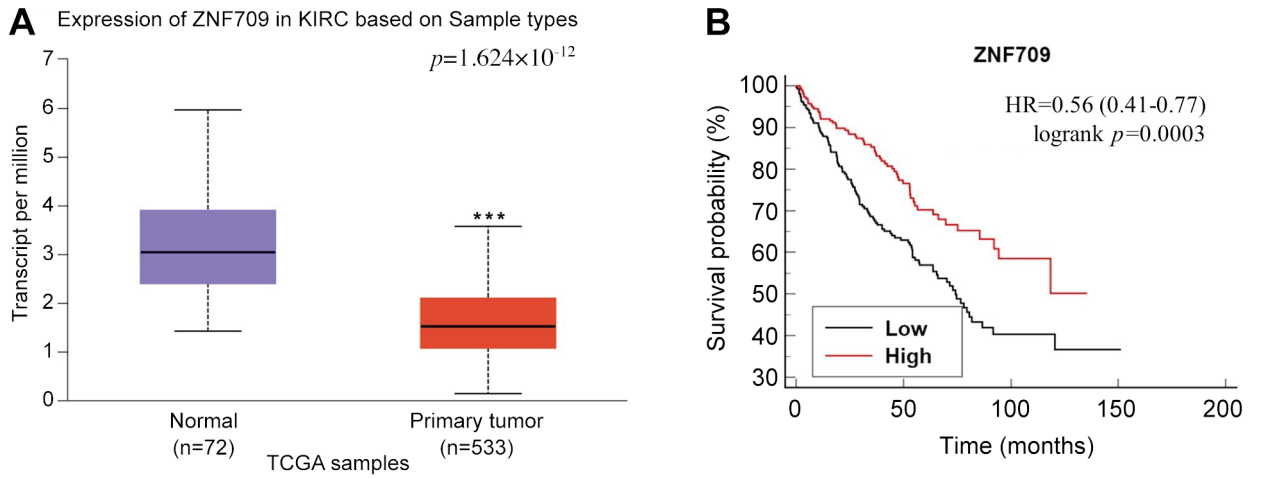

Figure 19. *Differential expression of KRAB zinc finger protein 709 (ZNF709). A: mRNA expression of ZNF709 in normal and clear cell renal carcinoma tumors. B: Kaplan-Meier survival plot for ZNF709 high expression and low expression groups. K-M plot was generated using the MedCalc statistical software. *** denotes the statistical significance of p<0.001.*

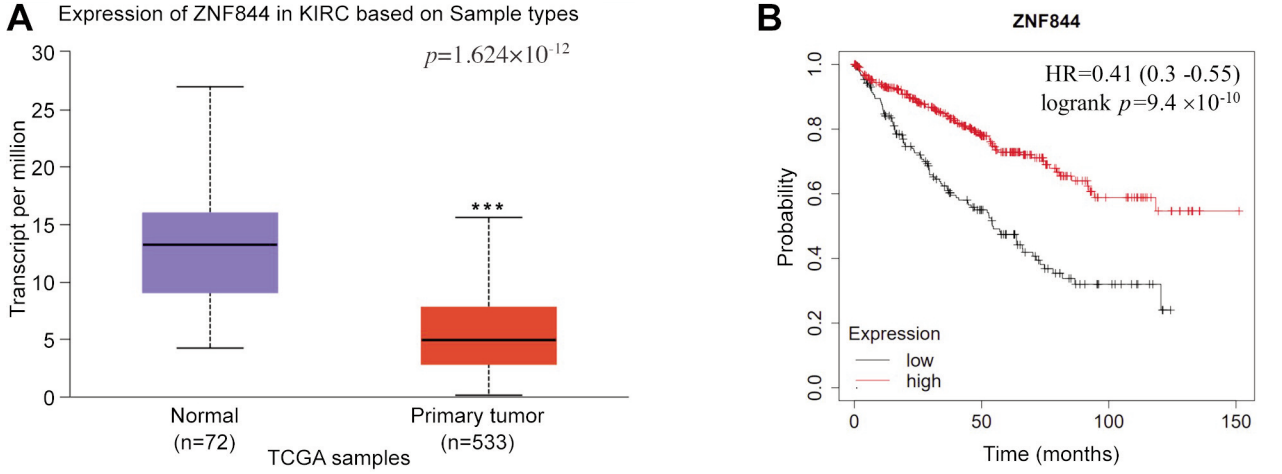

Figure 20. *Differential expression of KRAB zinc finger proteins 844 (ZNF844). Located on Chromosome 19p13.2. Kaplan Meier plots were generated either using the KM plotter A: mRNA expression of ZNF844 in normal and clear cell renal carcinoma tumors. B: Kaplan-Meier survival plot for ZNF844 high expression and low expression groups. K-M plot was generated using the KM plotter web tool. *** denotes the statistical significance of p<0.001. The AUC was 0.642, 95% CI=0.599 to 0.683.*

system pathway) with the most significant immune pathway in the Reactome database being antigen-processing cross-presentation (R-HSA-1236975; $p<1\times10^{-20}$, FDR<0.001, NES=–2.1904). GSEA analysis of the GO Biological Processes, KEGG, and Reactome databases did not reveal any significantly enriched pathways among the genes positively correlated with ZNF844 expression.

The ORA method was also used to identify over-represented pathways among negatively correlated genes. The ORA method also yielded similar results whereby 14 out of the 20 topmost enriched pathways are immune related pathways. These included GO:0006955-immune response (FDR<1×10^{-20}, $p<1\times10^{-20}$, enrichment ratio=1.3643), GO:0006952-defense response (FDR£1×10^{-20}, $p<1\times10^{-20}$, enrichment ratio=1.2939), GO:0034097-response to cytokine (FDR£0.001, p<1E-20, enrichment ratio=1.3397), GO:0019221-cytokine-mediated signaling pathway (FDR<1×10^{-20}, $p<1\times10^{-20}$, enrichment ratio=1.4676), GO:0050776: regulation of immune response (FDR=2.22×10^{-16}, $p=2.82\times10^{-13}$, enrichment ratio=1.3634), GO:0045087-innate immune response (FDR=4.32×10^{-15}, $p=3.67\times10^{-12}$, enrichment ratio=1.3683), GO:0045321-leukocyte activation (FDR=4.21×10^{-15}, $p=3.67\times10^{-12}$, enrichment ratio=1.2977), GO:0002252-immune effector process (FDR=2.14×10^{-14}, $p=1.61\times10^{-11}$, enrichment

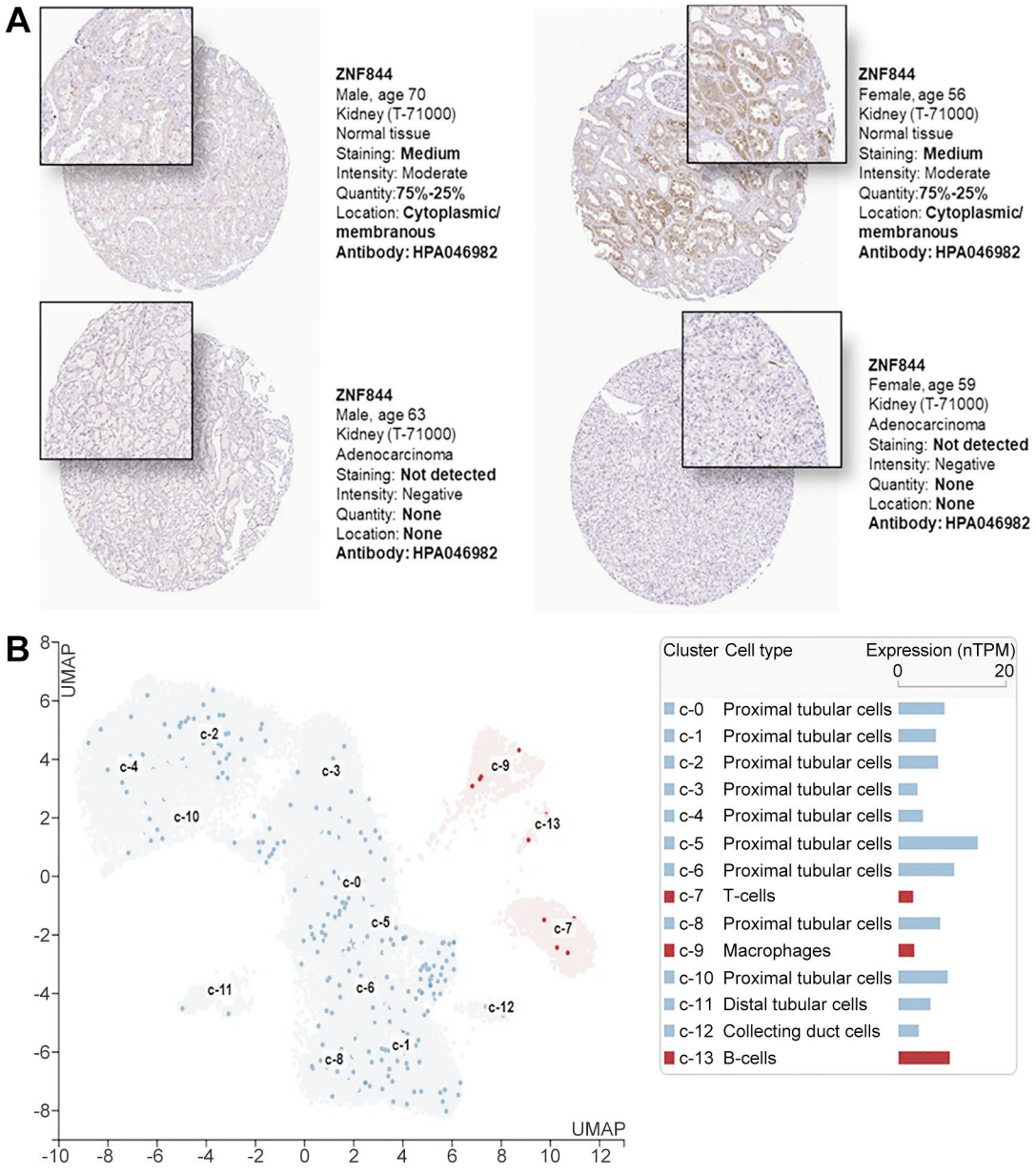

Figure 21. *Continued*

ratio=1.29610), GO:0006954-inflammatory response (FDR=6.39×10^{14}, p=4.28×10^{-11}, enrichment ratio=1.3725) and GO:0006959-humoral immune response (FDR= 8.63×10^{-14}, p=5.37×10^{-11}, enrichment ratio=1.6696). Table III presents the top 20 most enriched pathways based on (FDR value) among inversely correlated genes.

ZNF844 expression and tumor microenvironment. The consistency of both GSEA and ORA methods with regards to the immune-related pathways being highly enriched among negatively correlated genes suggests that ZNF844 may be associated with immune function and tumor microenvironment. More specifically, data indicates that there is an inverse relationship between immune system function and ZNF844 expression, whereby down-regulation of ZNF844 is associated with activation of the immune system. Therefore, we analyzed ZNF844 transcript levels in relationship to immune cell infiltration within the context of the ccRCC tumor microenvironment (Figure 24A and B). We focused on T-cells, B-cells (Figure 24A), and antigen-presenting cells (macrophages and dendritic cells) (Figure 24B) infiltrates because most of the enriched pathways associated with ZNF844

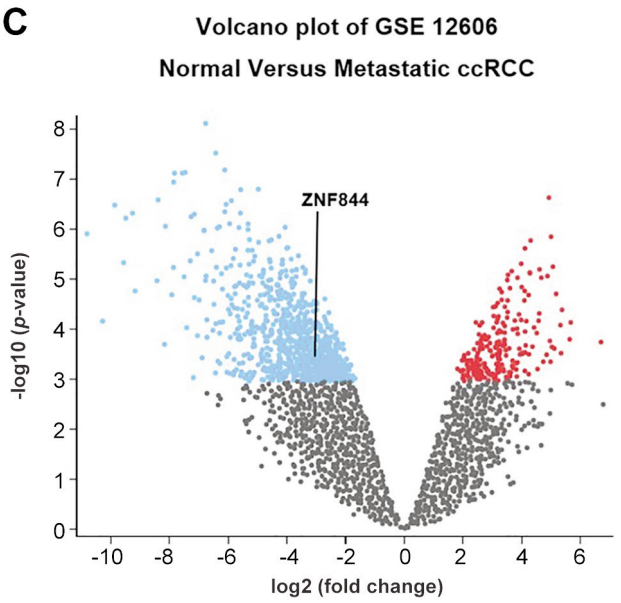

Figure 21. *ZNF844 protein and RNA expression in renal tissue. A: Immunohistochemistry images from the Human Protein Atlas demonstrate the expression of ZNF844 protein in normal and renal cancer tissues. B: Gene cluster map (from Human Protein Atlas) of cell types expressing ZNF844 in the Kidneys. ZNF844 is primarily expressed in the epithelial cells of proximal convoluted tubules (PCT) and immune cells (B-cells, T-cell and macrophages) within the Kidney. ZNF844 expression is highest in c5-gene cluster of the PCT. The Human Protein Atlas website (https://www.proteinatlas.org/) was accessed in May 2021 (Figure 21A) and on February 2, 2022 (Figure 21B). C: Volcano plot of GSE12606 dataset from NCBI GEO. ZNF844 expression was reduced in patients with clear cell renal carcinoma [log2 fold change=–2.905, -log10(p-Value)=3.574]. Blue dots represent genes significantly down-regulated (adjusted p<0.05) while ret dots represents genes significantly up-regulated in clear cell renal carcinoma relative to normal tissue (adjusted p<0.05).*

Table I. *Clinicopathological Features of ccRCC TCGA KIRC dataset downloaded from UCSC Xena web tool. One way-ANOVA was used to analyze ZNF844 gene expression across clinicopathological features. T-test was conducted to analyze differential gene expression of ZNF844 between sex. Statistical significance was set at p<0.05.*

Clinicopathological features	n	Statistics
Sex		p=0.838
Male	385	
Female	188	
Histological grade		p<0.001
Normal	72	
1	12	
2	216	
3	206	
4	70	
Pathological stage		p<0.001
Normal	72	
1	267	
2	57	
3	121	
4	84	
Metastasis		p<0.001
Normal	72	
N0	240	
N1	16	
Age		p=0.442
21-40 years	27	
41-60 years	237	
61-80 years	244	
81+ years	25	

Table II. *Univariate and multivariant Cox regression analysis of demographics, clinicopathological features, and ZNF844 expression in relation to overall survival in ccRCC patients. The statistical significance was set at p<0.05.*

Clinico-pathological features	Univariate analysis HR (95%CI) p-Value	Multivariate analysis HR (95%CI) p-Value
Sex	0.9495 (0.6979 to 1.2917) p=0.7412	0.5372 (0.6612 to 1.2406) p=0.9057
Age	1.7713 (1.3045 to 2.4050) p=0.0002	1.4909 (1.0915 to 2.0363) p=0.0121
Stage	3.8325 (2.7953 to 5.2547) p<0.0001	3.3757 (2.4442 to 4.6623) p<0.0001
Grade	1.1885 (0.8793 to 1.6064) p=0.2612	0.8313 (0.6069 to 1.1386) p=0.2496
ZNF844 expression	0.4128 (0.2994 to 0.5690) p<0.0001	0.5141 (0.3668 to 0.7204) p=0.0001

expression were primarily related to adaptive immune system function. ZNF844 showed negligible to weak, negative correlations with CD4-Th2, CD4 memory, CD8 cells, B-cells, and naïve CD4 infiltrates (Figure 24A). Weak to negligible correlations were also noted for antigen-presenting cell infiltrates (Figure 24B). However, ZNF844 expression did show moderate negative correlations (R=–0.558, $p=5.15\times10^{-39}$) with CD4-Th1 infiltrates (Figure 24A). To further explore this observation, we conducted a correlation analysis between ZNF844 expression and several T-cell signatures (Figure 24C). The strongest correlations were seen between ZNF844 and TH1-like T-cells (R= -0.36, $p=3.7\times10^{-19}$) and between ZNF844 and exhausted T-cell signatures (R=–0.37, $p=4.1\times10^{-21}$). This data further suggests a role for ZNF844 in immune function.

Expression profile of ZNF844 in different cancers. Finally, we examined ZNF844 expression across cancer types (Figure 25 and Table IV). ZNF844 was significantly down-regulated (p<0.05) in breast, cervical, colon, esophageal, head and neck, clear cell renal carcinoma, renal papillary, lung, prostate, rectal, thyroid, and uterine cancers (Figure 25). The

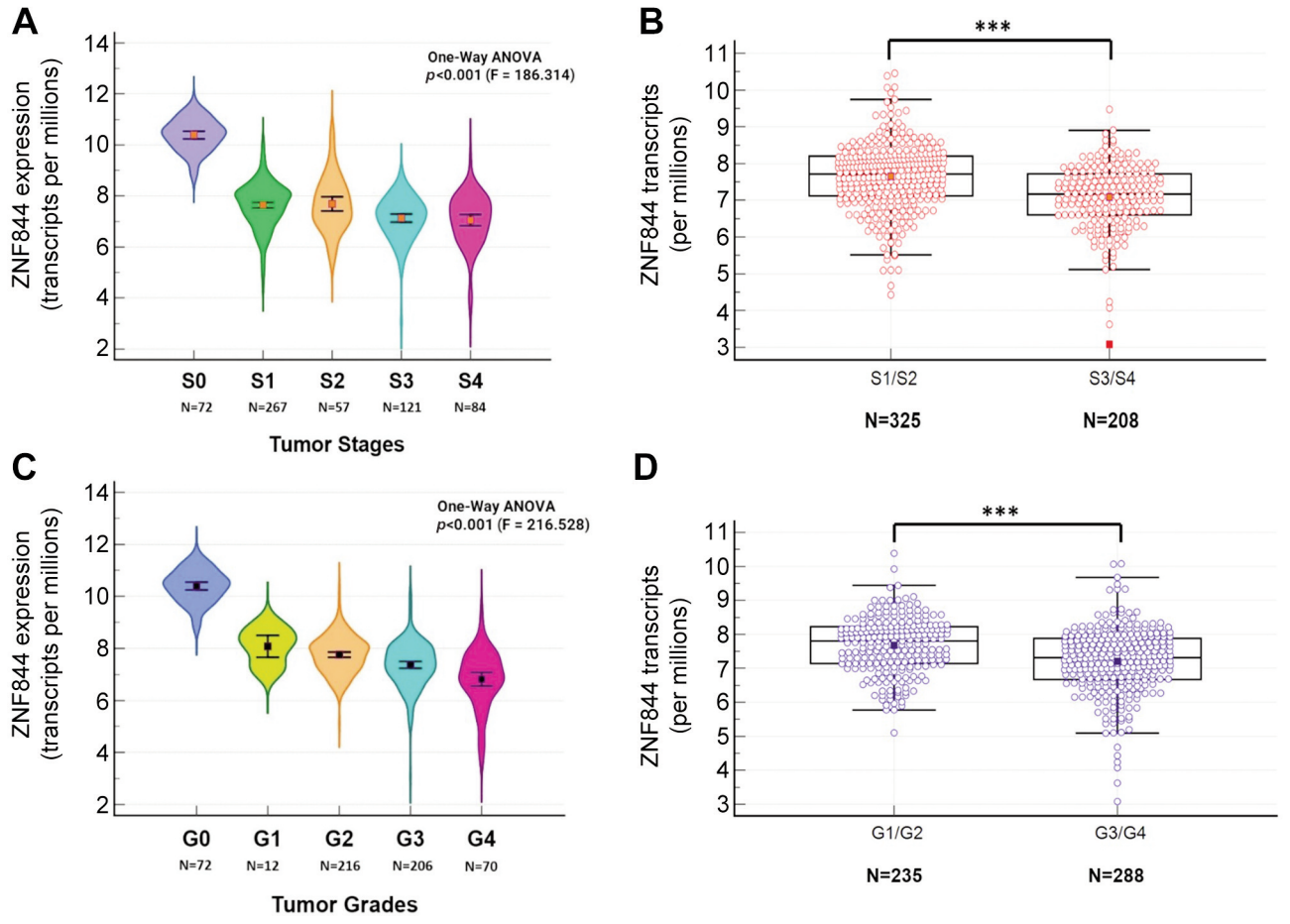

Figure 22. *Clinicopathological features of ZNF844 expression in clear cell renal carcinoma. Plots were created by UALCAN analysis of RNAseq data from TCGA data sets or from TCGA datasets downloaded from the USCS Xena website. A: Expression of ZNF844 transcripts at various cancer stages in clear cell renal carcinoma. One Way ANOVA was utilized to determine statistical significance of ZNF844 across stages. ZNF844 transcripts levels were significantly diminished in all tumor stages relative to normal tissues [F(4, 596)=186.314, df=4, p<0.001]. Tukey-Kramer multiple comparison test showed differences between S0 vs. S1, S2, S3 and S4 (p<0.05); S1 vs. S3 and S4 (p<0.05); S2 vs. S3 and S4 (p<0.05). B: Comparison of ZNF844 expression in lower stages (S1+S2) vs. higher stages (S3+S4) using Student t-test. Gene expression was significantly lower (p<0.001) in advanced stages (stages 3 and 4). C: Expression of ZNF844 transcripts at various histological grades of clear cell renal carcinoma. One-way ANOVA was utilized to determine statistical significance of ZNF844 across grades. ZNF844 transcripts levels were significantly diminished in all tumor grades relative to normal tissues [F(4, 571)=216.528, df=4, p<0.001]. Tukey-Kramer multiple comparison test showed differences between G0 vs. G1, G2, G3 and G4 (p<0.05); G1 vs. G3 and G4 (p<0.05); G2 vs. G3 and G4 (p<0.05); G3 vs. G1 and G2 (p<0.05). D: Comparison of ZNF844 expression in lower grades (G1+G2) vs. higher grades (G3+G4) using Students t-test. ZNF844 transcripts were significantly reduced in all tumor grades relative to normal tissues. Higher histological grades (grades 3 and 4) had significantly lower (p<0.001) levels of ZNF844 transcripts. (***p<0.001; **p<0.01; *p<0.05).*

greatest degree of significance was seen in renal papillary and clear cell carcinomas. In terms of overall survival, changes in ZNF844 expression were only associated with survival in patients with ccRCC and head and neck squamous cell carcinoma (HNSCC) (Table IV).

Discussion

Though poorly understood, it is becoming increasingly clear that KRAB-ZFPs play a major role in the development of cancer and tumor progression (9, 30). The ubiquitous nature of the KRAB-ZFPs, which constitute the largest family of transcription factors, have prevented in-depth analysis of how these proteins contribute or prevent tumorigenesis. KRAB-ZFPs are found on several chromosomes. Clusters of closely related ZFPs are located on chromosomes 4, 7, 8, 10, 19, with the largest clusters located on the p and q arms of chromosome 19 (6, 31-35). We recently reported that ZNF433, a KRAB-ZFP located within a cluster found at chr19p13.2, is down-regulated in ccRCC, and its expression is closely associated with clinicopathological features of ccRCC (19). Given that there are several related KRAB-ZFPs

Table III. *Top 20 ORA enriched GO biological process pathways associated with genes inversely correlated with ZNF844 expression.*

Gene set	Pathway description	Enrichment score	*p*-Value	FDR (q-Value)
GO:0006955	Immune response	1.3643	$<1\times10^{-20}$	$<1\times10^{-20}$
GO:0006952	Defense response	1.2939	$<1\times10^{-20}$	$<1\times10^{-20}$
GO:0034097	Response to cytokine	1.3316	$<1\times10^{-20}$	$<1\times10^{-20}$
GO:0019221	Cytokine-mediated signaling pathway	1.4676	$<1\times10^{-20}$	$<1\times10^{-20}$
GO:0072599	Establishment of protein localization to endoplasmic reticulum	2.1120	$<1\times10^{-20}$	$<1\times10^{-20}$
GO:0045047	Protein targeting to ER	2.1659	$<1\times10^{-20}$	$<1\times10^{-20}$
GO:0006614	SRP-dependent cotranslational protein targeting to membrane	2.1807	$<1\times10^{-20}$	$<1\times10^{-20}$
GO:0006613	Cotranslational protein targeting to membrane	2.1196	1.11×10^{-16}	1.76×10^{-13}
GO:0071345	Cellular response to cytokine stimulus	1.3398	2.22×10^{-16}	2.82×10^{-13}
GO:0050776	Regulation of immune response	1.3634	2.22×10^{-16}	2.82×10^{-13}
GO:0002682	Regulation of immune system process	1.2862	3.33×10^{-16}	3.85×10^{-13}
GO:0070972	Protein localization to endoplasmic reticulum	1.9293	6.66×10^{-16}	7.06×10^{-13}
GO:0045321	Leukocyte activation	1.2977	4.21×10^{-15}	3.67×10^{-12}
GO:0001775	Cell activation	1.2786	4.32×10^{-15}	3.67×10^{-12}
GO:0045087	Innate immune response	1.3683	4.32×10^{-15}	3.67×10^{-12}
GO:0002443	Leukocyte mediated immunity	1.3684	1.97×10^{-14}	1.57×10^{-11}
GO:0002252	Immune effector process	1.2961	2.15×10^{-14}	1.61×10^{-11}
GO:0000184	Nuclear-transcribed mRNA catabolic process, nonsense-mediated decay	1.9488	3.37×10^{-14}	2.38×10^{-11}
GO:0006954	Inflammatory response	1.3725	6.39×10^{-14}	4.28×10^{-11}
GO:0006959	Humoral immune response	1.6696	8.63×10^{-14}	5.37×10^{-11}

in this region, we examined whether these proteins were also differentially expressed in clear cell renal carcinoma. Seventy percent (14 out of 20) were down-regulated similarly to ZNF433 (Table I). Moreover, decreases in the transcripts of ZNF20, ZNF426, ZNF440, ZNF441, ZNF442, ZNF443, ZNF561, ZNF564, ZNF709, and ZNF844 were associated with lower survival outcomes in ccRCC patients. This data suggests that downregulation of certain chr19.13.2 KRAB-ZFPs may represent a genomic signature for ccRCC.

Of the KRAB-ZFPs, ZNF844 was found to be exceptional because its expression, as well as its impact on survival outcome, had higher statistical relevance than other members of the chr19.13.2 cluster. Therefore, we examined ZNF844 expression in relation to the clinicopathological features of ccRCC. ZNF844 transcripts and proteins were found to be lower in renal carcinomas (See Figure 20, Figure 21A and C). Reductions in ZNF844 expression were closely associated with higher stage, grade, metastasis, as well as with unsatisfactory survival in ccRCC patients. Moreover, ZNF844 was shown to be an independent, moderate prognostic marker for overall survival. This data suggests that elevated or over-expression of ZNF844 has a protective effect against renal carcinomas and may act as a putative tumor suppressor gene.

Gene Set Enrichment Analysis of correlated genes indicated that immune-related pathways were over-represented in an inverse manner (Figure 23C-E), thereby suggesting that ZNF844 is associated with the regulation of the immune system. This supposition is corroborated by earlier reports that clusters of KRAB-ZFPs located on

Table IV. *Expression profile of ZNF844 in different cancers. Values were obtained from TIMER 2.0.*

Tumor	Change inZNF 844 transcript expression	*p*-Value	Effect of differential expression on overall survival
BLCA	Down-regulation	0.120015	$p>0.05$
BRCA	Down-regulation	2.09×10^{-6}	$p>0.05$
CESC	Down-regulation	0.035041	$p>0.05$
COAD	Down-regulation	2.62×10^{-15}	$p>0.05$
ESCA	Down-regulation	0.004057	$p>0.05$
GBM	Up-regulation	0.044816	$p>0.05$
HNSC	Down-regulation	1.56×10^{-15}	$p<0.01$*
KICH	Down-regulation	0.221509	$p>0.05$
KIRC	Down-regulation	1.34×10^{-25}	$p<0.01$*
KIRP	Down-regulation	1.61×10^{-8}	$p>0.05$
LIHC	Up-regulation	0.012234	$p>0.05$
LUAD	Down-regulation	5.74×10^{-6}	$p>0.05$
LUSC	Down-regulation	2.01×10^{-16}	$p>0.05$
PAAD	Down-regulation	0.243611	$p>0.05$
PCPG	Up-regulation	0.493265	$p>0.05$
PRAD	Down-regulation	0.001627	$p>0.05$
READ	Down-regulation	4.49×10^{-5}	$p>0.05$
STAD	Down-regulation	0.056518	$p>0.05$
THCA	Down-regulation	4.39×10^{-11}	$p>0.05$
UCEC	Down-regulation	1.46×10^{-10}	$p>0.05$

*Statistically significant. The overall survival value statistic describes whether changes in ZNF844 expression in cancer patients were associated with changes in survival outcomes. *denotes reductions in gene expression relative to normal tissue were associated with significantly poorer overall survival.

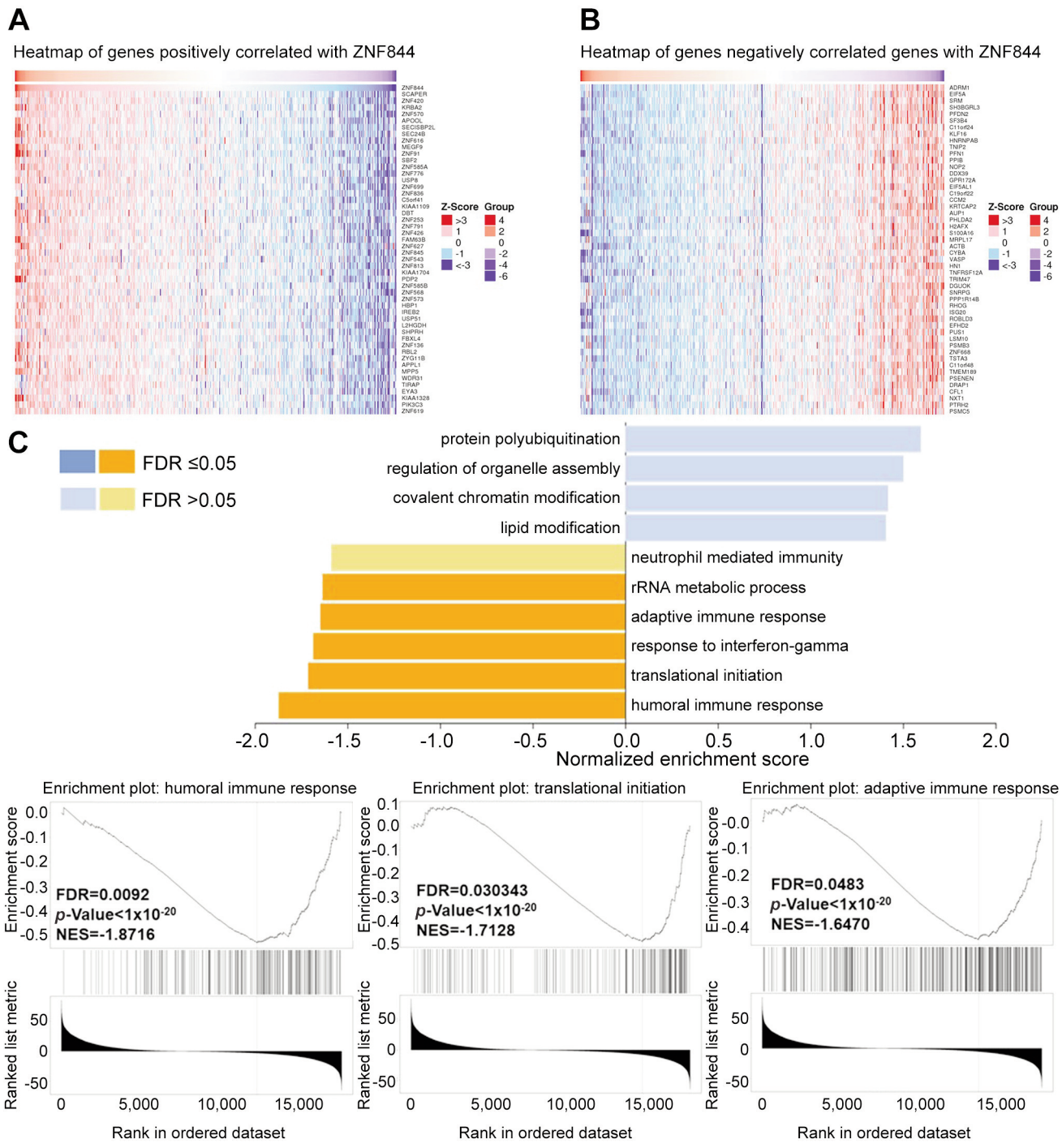

Figure 23. *Continued*

chromosome 19 are highly expressed in human T-lymphocytes (31). Indeed, analysis of immune infiltrates in ccRCC revealed that ZNF844 expression correlates moderately and inversely but in a highly significant manner to TH_1 $CD4^+$ T-lymphocytes activity (Figure 24A). Conversely, ZNF844 expression is only negligibly associated with other types of lymphocytes (B-cells) or myeloid lineage cells (Figure 24B). However, Figure 24D does suggest ZNF844 expression is highest in naïve B-cell cells in comparison to other immune cells. This discrepancy may be due to the markers utilized to identify the naïve B-cell subtype across different databases. An additional explanation is that differences in tissue (in this

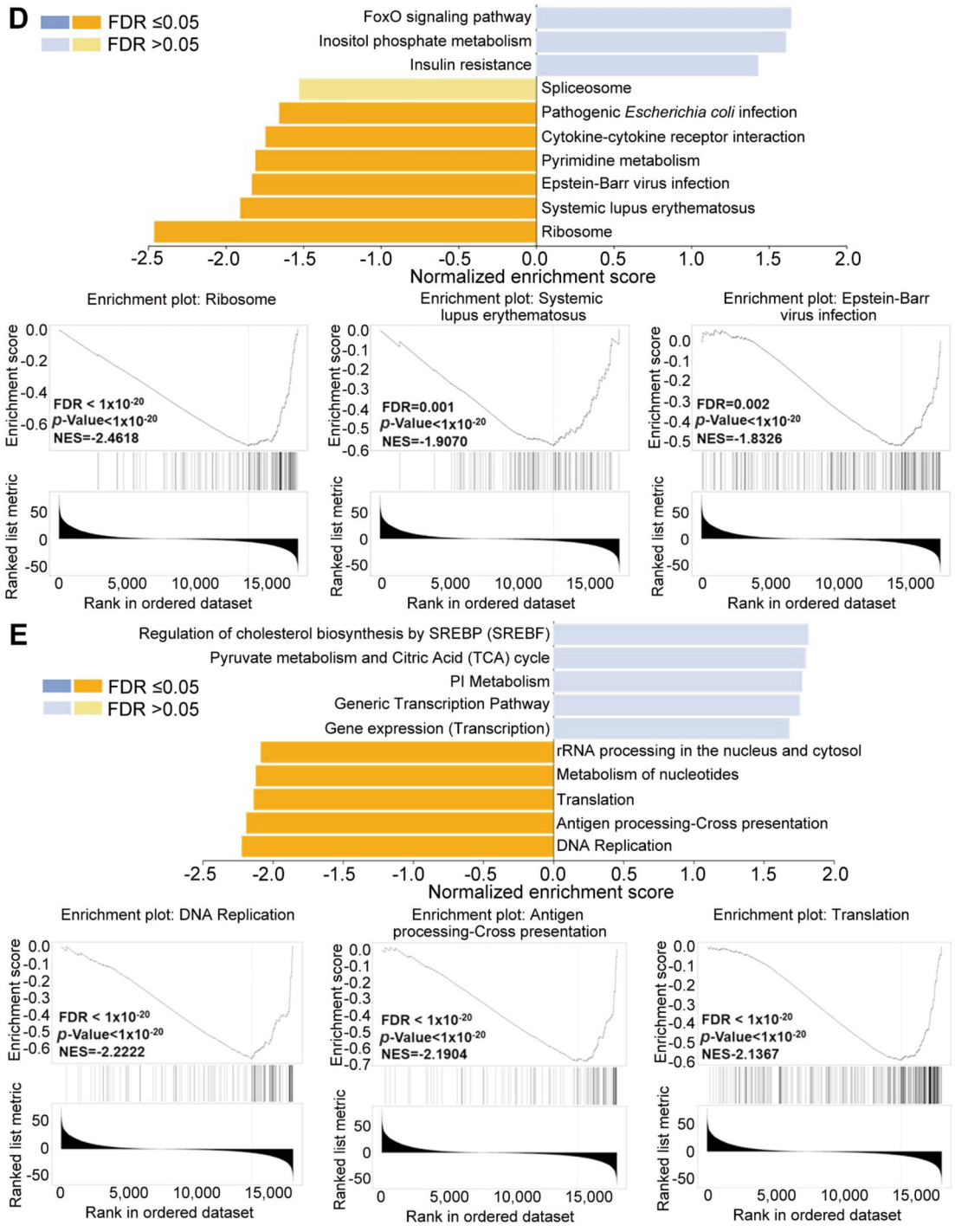

Figure 23. *Enrichment pathway analysis of genes co-expressed with ZNF844. A: Heat maps of the negatively correlated genes associated with ZNF844 B: Heat map of the positively correlated genes associated with ZNF844 expression. C: GSEA Pathway analysis of the GO Biological Process database for genes co-expressed with ZNF844. Enrichment plots are provided for the topmost significant pathways that were over-represented among the inversely correlated genes. D: GSEA Pathway analysis of the GSEA KEGG database for genes co-expressed with ZNF844. Enrichment plots are provided for the topmost significant pathways that were over-represented. E: GSEA Pathway analysis Reactome database for genes co-expressed with ZNF844. Enrichment plots are also provided for the topmost significant pathways that were over-represented among genes inversely correlated with ZNF844. The weight set cover analysis feature was utilized to minimize pathway redundancies. Blue-colored bars represent pathways enriched in positively correlated genes. The dark blue bars indicate that the FDR (q value) is <0.05 whereas, the light blue bars indicate that the pathways with FDR (q value) >0.05. Orange colored bars represent pathways enriched in inversely correlated genes, with dark orange bars depicting pathways with FDR <0.05, whereas the light orange bars represent pathways with FDR >0.05.*

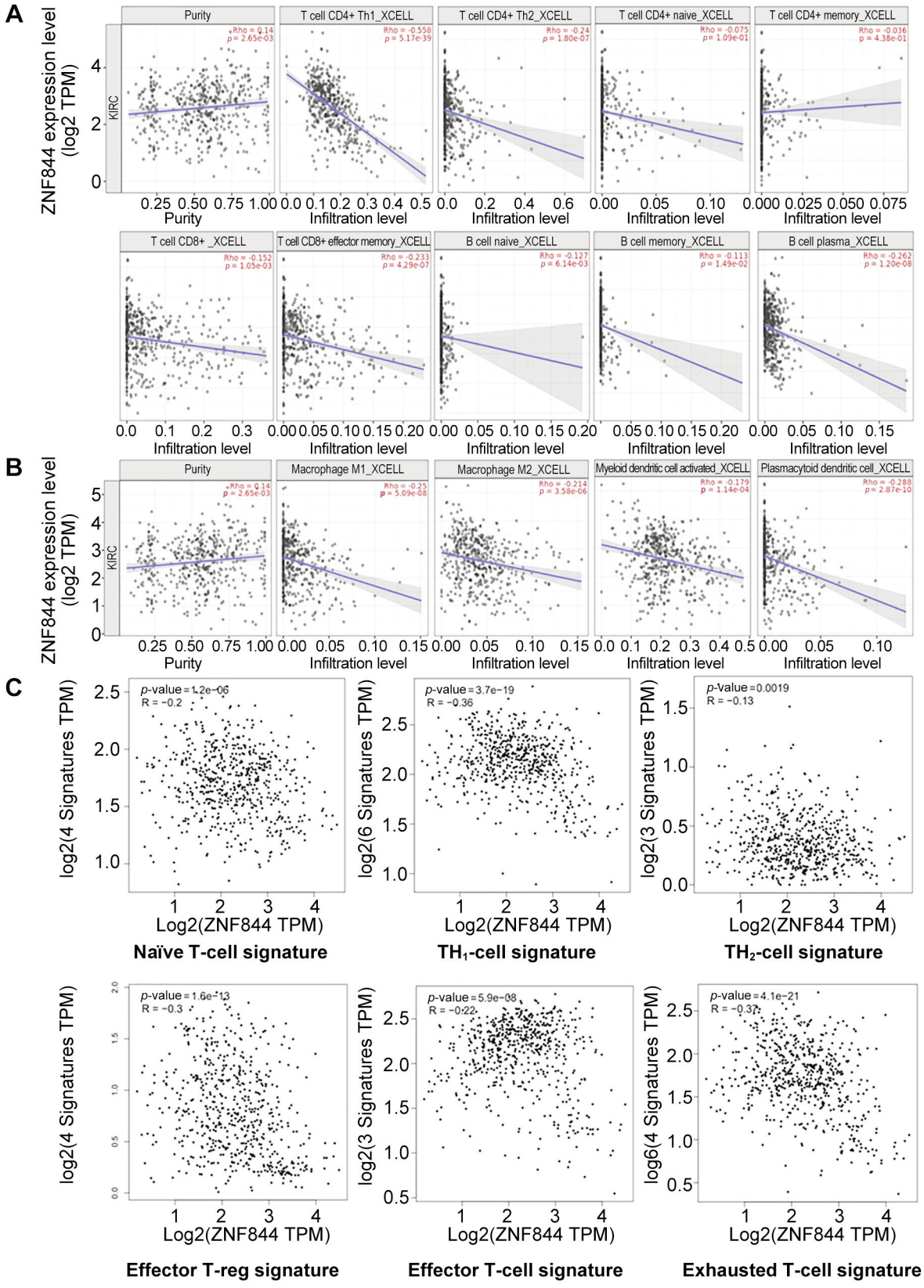

Figure 24. *Continued*

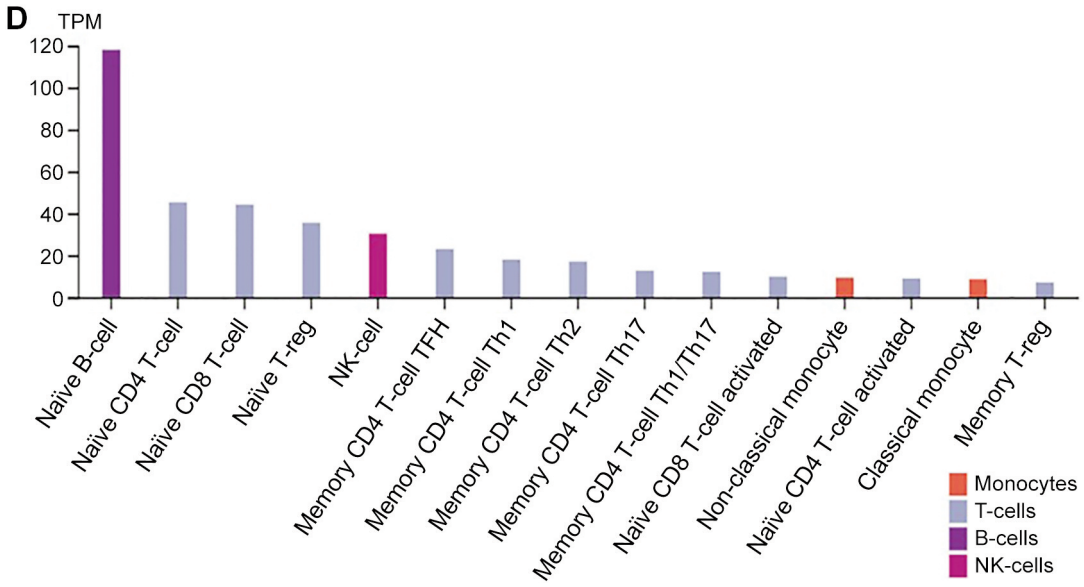

Figure 24. *Correlation analysis of ZNF844 expression with immune cell infiltration and the tumor microenvironment in clear cell renal carcinoma. Scatter plots were generated using Timer 2.0. A: ZNF844 expression in relationship to B and T-cell infiltrates. B: ZNF844 expression relative to antigen-presenting cells (APC) infiltrate. C: Correlation analysis between ZNF844 and key T-cell signatures associated with tumor microenvironment in clear cell renal carcinoma. Statistical significance was determined with Spearman's rank correlation for Figure 24A and B and Pearson's coefficient for Figure 24C. D: Single cell ZNF844 expression in naïve and activated immune cells. Data is derived from Human Protein Atlas analysis of the Schmiedel dataset.*

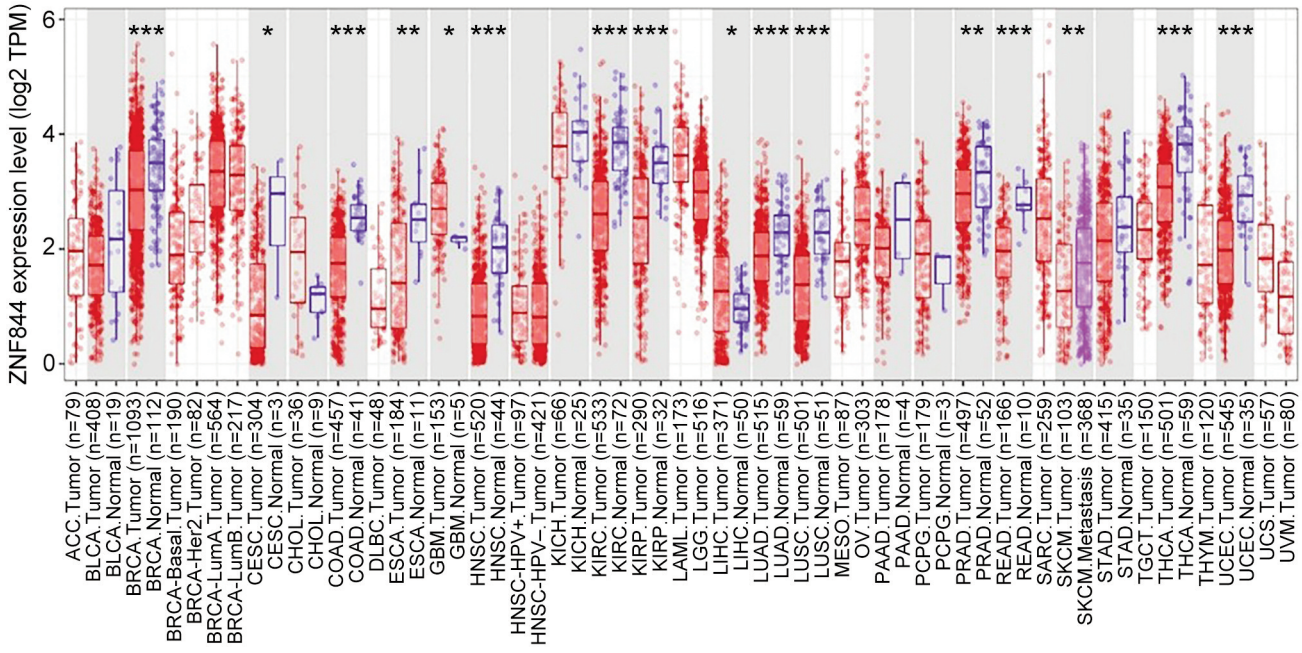

Figure 25. *Expression profile of ZNF844 in Different Cancers. The graph was generated by TIMER 2.0. The statistical significance is computed by comparing gene expression to normal tissue, in particular cancer. * denotes changes in gene expression relative to normal tissue are significantly different. ACC: Adrenocortical carcinoma; BLCA: bladder urothelial carcinoma; BRCA: breast invasive carcinoma; CESC: cervical squamous cell carcinoma and endocervical adenocarcinoma; CHOL: cholangiocarcinoma; COAD: colon adenocarcinoma; ESCA: esophageal carcinoma; GBM: glioblastoma multiforme; HNSC: head and neck squamous cell carcinoma; KICH: kidney chromophobe; KIRC: kidney renal clear cell carcinoma; KIRP: kidney renal papillary cell carcinoma; LIHC: liver hepatocellular carcinoma; LUAD: lung adenocarcinoma; LUSC: lung squamous cell carcinoma; PAAD: pancreatic adenocarcinoma; PCPG: pheochromocytoma and paraganglioma; PRAD: prostate adenocarcinoma; READ: rectum adenocarcinoma; STAD: stomach adenocarcinoma; THCA: thyroid carcinoma; UCEC: uterine corpus endometrial carcinoma.*

case non-cancerous renal tissue for Figure 24D) could dictate which genes are expressed. Nonetheless, Figure 24D further supports the observations that ZNF844 is associated with immune cell function.

It should be noted that renal carcinoma is highly enriched with immune cells; particularly T-lymphocytes such as the Th1 lineage (36-40). The Th1 lymphocyte phenotype is generally understood to promote anti-tumor immunity and thus is associated with more favorable outcomes in patients with renal carcinomas (40). Conversely, high levels of specific subsets of CD8+, T-regs, and tumor-associated macrophages are associated with unfavorable prognosis in ccRCC (41-45). The high level of T-cell infiltrates is utilized as the basis for the use of PDL1 and checkpoint inhibitors to attenuate; presumably, T-cell inhibition, exhaustion, and anergy, as well as tumor immune evasion in metastatic renal carcinoma (37, 46-49). Our observations indicate that down-regulation of ZNF844 is associated with more advanced disease with poor outcomes and increases in the anti-tumor (Th1) lymphocytic phenotype. These seemingly contradictory results probably suggest that ZNF844 downregulation may be associated with T-cell dysfunction or T-cell exhaustion. In fact, an examination of the relationship between ZNF844 with different T-cell signatures (Figure 24C) revealed that ZNF844 expression had the strongest inverse correlation as well as statistical relevance with the exhausted T-cell phenotype. Moreover, Figure 24D suggest that ZNF844 expression lower in activated lymphocytes, further suggesting that a loss of ZNF844 function is associated with immune cell activation.

Finally, we examined ZNF844 expression in relation to other cancers to determine whether this protein was a possible pan-cancer biomarker (Figure 25 and Table IV). Though the transcription factor was differentially expressed in numerous cancers, the most significant statistical relevance with regards to gene expression and overall survival occurred in ccRCC patients (Table IV). A similar pattern but less statistically robust effect was observed in head and neck squamous cell carcinomas (HNSCC). Hence, ZNF844 prognostic value regarding cancer is primarily limited to ccRCC and possibly HNSCC.

Conclusion

In summary, KRAB-ZFPs gene expression appears to be dysregulated in ccRCC and may represent a genomic signature of ccRCC. We have identified KRAB zinc finger protein ZNF844 as a potential predictive biomarker that may also act as a tumor suppressor in clear cell carcinoma. *In silico* analysis suggests that down-regulation of ZNF844 is associated with advanced clinicopathological features of ccRCC and poorer patient survival. ZNF844 is more closely associated with the inverse expression of several immune-related pathways, the helper T-cell subtype 1 signature, and the exhausted T-cell phenotype. Our observations therefore suggest that reduction in ZNF844 transcripts correlates with the activation of certain elements of the immune system as the renal carcinoma progresses to advanced stages. However, a weakness of this study is that these observations are made *via in silico* analysis. Moreover, protein expression data reflects a qualitative assessment of representative immunohistochemistry images. Further investigations in cellular and tumor models are warranted to validate these observations. In addition, functional studies are required to ascertain the role of ZNF844 in ccRCC tumor pathology and to identify the gene targets of this novel transcription factor. Nonetheless, our observations indicate that ZNF844 is indeed a biomarker for ccRCC. Moreover, our study suggests novel roles for KRAB-ZFP in the modulation of cellular functions in ccRCC.

Conflicts of Interest

The funders had no role in the design of the study; in the collection, analyses, or interpretation of data; in the writing of the manuscript, or in the decision to publish the results.

Authors' Contributions

The Authors contributed to the preparation in the following ways: Conceptualization, SOH, MDS, and RRR; methodology, SOH; resources, KFAS; writing—original draft preparation, SOH; writing—review and editing, KFAS, RRR, MDS; funding acquisition, KFAS. All Authors have read and agreed to the published version of the manuscript.

Acknowledgements

This research was supported by the National Institute of Minority Health and Health Disparities of the National Institutes of Health through Grant Number U54 MD 007582 and by the National Cancer Institute of the NIH through Grant Number U54CA233396.

References

1 Eble JN, Sauter G, Epstein JI and Sesterhenn IA: Renal cell carcinoma. In: World Health Organization Classification of Tumours. Pathology and Genetics of Tumours of the Urinary System and Male Genital Organs. Lyon, France, IARC Press, pp 8-14, 2004.

2 Siegel RL, Miller KD and Jemal A: Cancer statistics, 2019. CA Cancer J Clin *69(1)*: 7-34, 2019. PMID: 30620402. DOI: 10.3322/caac.21551

3 Low G, Huang G, Fu W, Moloo Z and Girgis S: Review of renal cell carcinoma and its common subtypes in radiology. World J Radiol *8(5)*: 484-500, 2016. PMID: 27247714. DOI: 10.4329/wjr.v8.i5.484

4 Urrutia R: KRAB-containing zinc-finger repressor proteins. Genome Biol *4(10)*: 231, 2003. PMID: 14519192. DOI: 10.1186/gb-2003-4-10-231

5 Sobocińska J, Molenda S, Machnik M and Oleksiewicz U: KRAB-ZFP transcriptional regulators acting as oncogenes and

tumor suppressors: an overview. Int J Mol Sci *22(4)*: 2212, 2021. PMID: 33672287. DOI: 10.3390/ijms22042212

6 Huntley S, Baggott DM, Hamilton AT, Tran-Gyamfi M, Yang S, Kim J, Gordon L, Branscomb E and Stubbs L: A comprehensive catalog of human KRAB-associated zinc finger genes: insights into the evolutionary history of a large family of transcriptional repressors. Genome Res *16(5)*: 669-677, 2006. PMID: 16606702. DOI: 10.1101/gr.4842106

7 Yang L, Hamilton SR, Sood A, Kuwai T, Ellis L, Sanguino A, Lopez-Berestein G and Boyd DD: The previously undescribed ZKSCAN3 (ZNF306) is a novel "driver" of colorectal cancer progression. Cancer Res *68(11)*: 4321-4330, 2008. PMID: 18519692. DOI: 10.1158/0008-5472.CAN-08-0407

8 Imbeault M, Helleboid PY and Trono D: KRAB zinc-finger proteins contribute to the evolution of gene regulatory networks. Nature *543(7646)*: 550-554, 2017. PMID: 28273063. DOI: 10.1038/nature21683

9 Oleksiewicz U, Gładych M, Raman AT, Heyn H, Mereu E, Chlebanowska P, Andrzejewska A, Sozańska B, Samant N, Fąk K, Auguścik P, Kosiński M, Wróblewska JP, Tomczak K, Kulcenty K, Płoski R, Biecek P, Esteller M, Shah PK, Rai K and Wiznerowicz M: TRIM28 and interacting KRAB-ZNFs control self-renewal of human pluripotent stem cells through epigenetic repression of pro-differentiation genes. Stem Cell Reports *9(6)*: 2065-2080, 2017. PMID: 29198826. DOI: 10.1016/j.stemcr.2017.10.031

10 Quenneville S, Verde G, Corsinotti A, Kapopoulou A, Jakobsson J, Offner S, Baglivo I, Pedone PV, Grimaldi G, Riccio A and Trono D: In embryonic stem cells, ZFP57/KAP1 recognize a methylated hexanucleotide to affect chromatin and DNA methylation of imprinting control regions. Mol Cell *44(3)*: 361-372, 2011. PMID: 22055183. DOI: 10.1016/j.molcel.2011.08.032

11 Lupo A, Cesaro E, Montano G, Zurlo D, Izzo P and Costanzo P: KRAB-Zinc finger proteins: a repressor family displaying multiple biological functions. Curr Genomics *14(4)*: 268-278, 2013. PMID: 24294107. DOI: 10.2174/1389202911314999002

12 Canzian F, Amati P, Harach HR, Kraimps JL, Lesueur F, Barbier J, Levillain P, Romeo G and Bonneau D: A gene predisposing to familial thyroid tumors with cell oxyphilia maps to chromosome 19p13.2. Am J Hum Genet *63(6)*: 1743-1748, 1998. PMID: 9837827. DOI: 10.1086/302164

13 Trojan J, Brieger A, Raedle J, Esteller M and Zeuzem S: 5'-CpG island methylation of the LKB1/STK11 promoter and allelic loss at chromosome 19p13.3 in sporadic colorectal cancer. Gut *47(2)*: 272-276, 2000. PMID: 10896921. DOI: 10.1136/gut.47.2.272

14 Bolton KL, Tyrer J, Song H, Ramus SJ, Notaridou M, Jones C, Sher T, Gentry-Maharaj A, Wozniak E, Tsai YY, Weidhaas J, Paik D, Van Den Berg DJ, Stram DO, Pearce CL, Wu AH, Brewster W, Anton-Culver H, Ziogas A, Narod SA, Levine DA, Kaye SB, Brown R, Paul J, Flanagan J, Sieh W, McGuire V, Whittemore AS, Campbell I, Gore ME, Lissowska J, Yang HP, Medrek K, Gronwald J, Lubinski J, Jakubowska A, Le ND, Cook LS, Kelemen LE, Brooks-Wilson A, Massuger LF, Kiemeney LA, Aben KK, van Altena AM, Houlston R, Tomlinson I, Palmieri RT, Moorman PG, Schildkraut J, Iversen ES, Phelan C, Vierkant RA, Cunningham JM, Goode EL, Fridley BL, Kruger-Kjaer S, Blaeker J, Hogdall E, Hogdall C, Gross J, Karlan BY, Ness RB, Edwards RP, Odunsi K, Moyisch KB, Baker JA, Modugno F, Heikkinenen T, Butzow R, Nevanlinna H, Leminen A, Bogdanova N, Antonenkova N, Doerk T, Hillemanns P, Dürst M, Runnebaum I, Thompson PJ, Carney ME, Goodman MT, Lurie G, Wang-Gohrke S, Hein R, Chang-Claude J, Rossing MA, Cushing-Haugen KL, Doherty J, Chen C, Rafnar T, Besenbacher S, Sulem P, Stefansson K, Birrer MJ, Terry KL, Hernandez D, Cramer DW, Vergote I, Amant F, Lambrechts D, Despierre E, Fasching PA, Beckmann MW, Thiel FC, Ekici AB, Chen X, Australian Ovarian Cancer Study Group, Australian Cancer Study (Ovarian Cancer), Ovarian Cancer Association Consortium, Johnatty SE, Webb PM, Beesley J, Chanock S, Garcia-Closas M, Sellers T, Easton DF, Berchuck A, Chenevix-Trench G, Pharoah PD and Gayther SA: Common variants at 19p13 are associated with susceptibility to ovarian cancer. Nat Genet *42(10)*: 880-884, 2010. PMID: 20852633. DOI: 10.1038/ng.666

15 Antoniou AC, Wang X, Fredericksen ZS, McGuffog L, Tarrell R, Sinilnikova OM, Healey S, Morrison J, Kartsonaki C, Lesnick T, Ghoussaini M, Barrowdale D, EMBRACE, Peock S, Cook M, Oliver C, Frost D, Eccles D, Evans DG, Eeles R, Izatt L, Chu C, Douglas F, Paterson J, Stoppa-Lyonnet D, Houdayer C, Mazoyer S, Giraud S, Lasset C, Remenieras A, Caron O, Hardouin A, Berthet P, GEMO Study Collaborators, Hogervorst FB, Rookus MA, Jager A, van den Ouweland A, Hoogerbrugge N, van der Luijt RB, Meijers-Heijboer H, Gómez García EB, HEBON, Devilee P, Vreeswijk MP, Lubinski J, Jakubowska A, Gronwald J, Huzarski T, Byrski T, Górski B, Cybulski C, Spurdle AB, Holland H, kConFab, Goldgar DE, John EM, Hopper JL, Southey M, Buys SS, Daly MB, Terry MB, Schmutzler RK, Wappenschmidt B, Engel C, Meindl A, Preisler-Adams S, Arnold N, Niederacher D, Sutter C, Domchek SM, Nathanson KL, Rebbeck T, Blum JL, Piedmonte M, Rodriguez GC, Wakeley K, Boggess JF, Basil J, Blank SV, Friedman E, Kaufman B, Laitman Y, Milgrom R, Andrulis IL, Glendon G, Ozcelik H, Kirchhoff T, Vijai J, Gaudet MM, Altshuler D, Guiducci C, SWE-BRCA, Loman N, Harbst K, Rantala J, Ehrencrona H, Gerdes AM, Thomassen M, Sunde L, Peterlongo P, Manoukian S, Bonanni B, Viel A, Radice P, Caldes T, de la Hoya M, Singer CF, Fink-Retter A, Greene MH, Mai PL, Loud JT, Guidugli L, Lindor NM, Hansen TV, Nielsen FC, Blanco I, Lazaro C, Garber J, Ramus SJ, Gayther SA, Phelan C, Narod S, Szabo CI, MOD SQUAD, Benitez J, Osorio A, Nevanlinna H, Heikkinen T, Caligo MA, Beattie MS, Hamann U, Godwin AK, Montagna M, Casella C, Neuhausen SL, Karlan BY, Tung N, Toland AE, Weitzel J, Olopade O, Simard J, Soucy P, Rubinstein WS, Arason A, Rennert G, Martin NG, Montgomery GW, Chang-Claude J, Flesch-Janys D, Brauch H, GENICA, Severi G, Baglietto L, Cox A, Cross SS, Miron P, Gerty SM, Tapper W, Yannoukakos D, Fountzilas G, Fasching PA, Beckmann MW, Dos Santos Silva I, Peto J, Lambrechts D, Paridaens R, Rüdiger T, Försti A, Winqvist R, Pylkäs K, Diasio RB, Lee AM, Eckel-Passow J, Vachon C, Blows F, Driver K, Dunning A, Pharoah PP, Offit K, Pankratz VS, Hakonarson H, Chenevix-Trench G, Easton DF and Couch FJ: A locus on 19p13 modifies risk of breast cancer in BRCA1 mutation carriers and is associated with hormone receptor-negative breast cancer in the general population. Nat Genet *42(10)*: 885-892, 2010. PMID: 20852631. DOI: 10.1038/ng.669

16 Teng BL, Hacker KE, Chen S, Means AR and Rathmell WK: Tumor suppressive activity of prolyl isomerase Pin1 in renal cell carcinoma. Mol Oncol *5(5)*: 465-474, 2011. PMID: 21764651. DOI: 10.1016/j.molonc.2011.06.002

17 Stevens KN, Fredericksen Z, Vachon CM, Wang X, Margolin S, Lindblom A, Nevanlinna H, Greco D, Aittomäki K, Blomqvist C, Chang-Claude J, Vrieling A, Flesch-Janys D, Sinn HP, Wang-

Gohrke S, Nickels S, Brauch H, GENICA Network, Ko YD, Fischer HP, Schmutzler RK, Meindl A, Bartram CR, Schott S, Engel C, Godwin AK, Weaver J, Pathak HB, Sharma P, Brenner H, Müller H, Arndt V, Stegmaier C, Miron P, Yannoukakos D, Stavropoulou A, Fountzilas G, Gogas HJ, Swann R, Dwek M, Perkins A, Milne RL, Benítez J, Zamora MP, Pérez JI, Bojesen SE, Nielsen SF, Nordestgaard BG, Flyger H, Guénel P, Truong T, Menegaux F, Cordina-Duverger E, Burwinkel B, Marmé F, Schneeweiss A, Sohn C, Sawyer E, Tomlinson I, Kerin MJ, Peto J, Johnson N, Fletcher O, Dos Santos Silva I, Fasching PA, Beckmann MW, Hartmann A, Ekici AB, Lophatananon A, Muir K, Puttawibul P, Wiangnon S, Schmidt MK, Broeks A, Braaf LM, Rosenberg EH, Hopper JL, Apicella C, Park DJ, Southey MC, Swerdlow AJ, Ashworth A, Orr N, Schoemaker MJ, Anton-Culver H, Ziogas A, Bernstein L, Dur CC, Shen CY, Yu JC, Hsu HM, Hsiung CN, Hamann U, Dünnebier T, Rüdiger T, Ulmer HU, Pharoah PP, Dunning AM, Humphreys MK, Wang Q, Cox A, Cross SS, Reed MW, Hall P, Czene K, Ambrosone CB, Ademuyiwa F, Hwang H, Eccles DM, Garcia-Closas M, Figueroa JD, Sherman ME, Lissowska J, Devilee P, Seynaeve C, Tollenaar RA, Hooning MJ, Andrulis IL, Knight JA, Glendon G, Mulligan AM, Winqvist R, Pylkäs K, Jukkola-Vuorinen A, Grip M, John EM, Miron A, Alnæs GG, Kristensen V, Børresen-Dale AL, Giles GG, Baglietto L, McLean CA, Severi G, Kosel ML, Pankratz VS, Slager S, Olson JE, Radice P, Peterlongo P, Manoukian S, Barile M, Lambrechts D, Hatse S, Dieudonne AS, Christiaens MR, Chenevix-Trench G, kConFab Investigators, AOCS Group, Beesley J, Chen X, Mannermaa A, Kosma VM, Hartikainen JM, Soini Y, Easton DF and Couch FJ: 19p13.1 is a triple-negative-specific breast cancer susceptibility locus. Cancer Res *72(7)*: 1795-1803, 2012. PMID: 22331459. DOI: 10.1158/0008-5472.CAN-11-3364

18 Xue Y, Meehan B, Fu Z, Wang XQD, Fiset PO, Rieker R, Levins C, Kong T, Zhu X, Morin G, Skerritt L, Herpel E, Venneti S, Martinez D, Judkins AR, Jung S, Camilleri-Broet S, Gonzalez AV, Guiot MC, Lockwood WW, Spicer JD, Agaimy A, Pastor WA, Dostie J, Rak J, Foulkes WD and Huang S: SMARCA4 loss is synthetic lethal with CDK4/6 inhibition in non-small cell lung cancer. Nat Commun *10(1)*: 557, 2019. PMID: 30718506. DOI: 10.1038/s41467-019-08380-1

19 Heyliger SO, Soliman KFA, Saulsbury MD and Reams RR: The identification of Zinc-finger protein 433 as a possible prognostic biomarker for clear-cell renal cell carcinoma. Biomolecules *11(8)*: 1193, 2021. PMID: 34439859. DOI: 10.3390/biom11081193

20 Chandrashekar DS, Bashel B, Balasubramanya SAH, Creighton CJ, Ponce-Rodriguez I, Chakravarthi BVSK and Varambally S: UALCAN: a portal for facilitating tumor subgroup gene expression and survival analyses. Neoplasia *19(8)*: 649-658, 2017. PMID: 28732212. DOI: 10.1016/j.neo.2017.05.002

21 Goldman MJ, Craft B, Hastie M, Repečka K, McDade F, Kamath A, Banerjee A, Luo Y, Rogers D, Brooks AN, Zhu J and Haussler D: Visualizing and interpreting cancer genomics data *via* the Xena platform. Nat Biotechnol *38(6)*: 675-678, 2020. PMID: 32444850. DOI: 10.1038/s41587-020-0546-8

22 Stickel JS, Weinzierl AO, Hillen N, Drews O, Schuler MM, Hennenlotter J, Wernet D, Müller CA, Stenzl A, Rammensee HG and Stevanović S: HLA ligand profiles of primary renal cell carcinoma maintained in metastases. Cancer Immunol Immunother *58(9)*: 1407-1417, 2009. PMID: 19184600. DOI: 10.1007/s00262-008-0655-6

23 Tang Z, Li C, Kang B, Gao G, Li C and Zhang Z: GEPIA: a web server for cancer and normal gene expression profiling and interactive analyses. Nucleic Acids Res *45(W1)*: W98-W102, 2017. PMID: 28407145. DOI: 10.1093/nar/gkx247

24 Tang Z, Kang B, Li C, Chen T and Zhang Z: GEPIA2: an enhanced web server for large-scale expression profiling and interactive analysis. Nucleic Acids Res *47(W1)*: W556-W560, 2019. PMID: 31114875. DOI: 10.1093/nar/gkz430

25 Zhang W, Zhang W, Gui L, Yan X, Zhou X, Ma Y, Yang Z, Fang Y, Zhang H and Shi J: Expression and prognosis of the B7 family in acute myeloid leukemia. Ann Transl Med *9(20)*: 1530, 2021. PMID: 34790736. DOI: 10.21037/atm-21-4255

26 Pontén F, Jirström K and Uhlen M: The Human Protein Atlas—a tool for pathology. J Pathol *216(4)*: 387-393, 2008. PMID: 18853439. DOI: 10.1002/path.2440

27 Li T, Fan J, Wang B, Traugh N, Chen Q, Liu JS, Li B and Liu XS: TIMER: A web server for comprehensive analysis of tumor-infiltrating immune cells. Cancer Res *77(21)*: e108-e110, 2017. PMID: 29092952. DOI: 10.1158/0008-5472.CAN-17-0307

28 Li T, Fu J, Zeng Z, Cohen D, Li J, Chen Q, Li B and Liu XS: TIMER2.0 for analysis of tumor-infiltrating immune cells. Nucleic Acids Res *48(W1)*: W509-W514, 2020. PMID: 32442275. DOI: 10.1093/nar/gkaa407

29 Vasaikar SV, Straub P, Wang J and Zhang B: LinkedOmics: analyzing multi-omics data within and across 32 cancer types. Nucleic Acids Res *46(D1)*: D956-D963, 2018. PMID: 29136207. DOI: 10.1093/nar/gkx1090

30 Pei L, He X, Li S, Sun R, Xiang Q, Ren G and Xiang T: KRAB zinc-finger protein 382 regulates epithelial-mesenchymal transition and functions as a tumor suppressor, but is silenced by CpG methylation in gastric cancer. Int J Oncol *53(3)*: 961-972, 2018. PMID: 29956735. DOI: 10.3892/ijo.2018.4446

31 Bellefroid EJ, Marine JC, Ried T, Lecocq PJ, Rivière M, Amemiya C, Poncelet DA, Coulie PG, de Jong P and Szpirer C: Clustered organization of homologous KRAB zinc-finger genes with enhanced expression in human T lymphoid cells. EMBO J *12(4)*: 1363-1374, 1993. PMID: 8467795.

32 Jackson MS, See CG, Mulligan LM and Lauffart BF: A 9.75-Mb map across the centromere of human chromosome 10. Genomics *33(2)*: 258-270, 1996. PMID: 8660974. DOI: 10.1006/geno.1996.0190

33 Shannon M, Ashworth LK, Mucenski ML, Lamerdin JE, Branscomb E and Stubbs L: Comparative analysis of a conserved zinc finger gene cluster on human chromosome 19q and mouse chromosome 7. Genomics *33(1)*: 112-120, 1996. PMID: 8617494. DOI: 10.1006/geno.1996.0166

34 Hamilton AT, Huntley S, Tran-Gyamfi M, Baggott DM, Gordon L and Stubbs L: Evolutionary expansion and divergence in the ZNF91 subfamily of primate-specific zinc finger genes. Genome Res *16(5)*: 584-594, 2006. PMID: 16606703. DOI: 10.1101/gr.4843906

35 Lorenz P, Dietmann S, Wilhelm T, Koczan D, Autran S, Gad S, Wen G, Ding G, Li Y, Rousseau-Merck MF and Thiesen HJ: The ancient mammalian KRAB zinc finger gene cluster on human chromosome 8q24.3 illustrates principles of C2H2 zinc finger evolution associated with unique expression profiles in human tissues. BMC Genomics *11*: 206, 2010. PMID: 20346131. DOI: 10.1186/1471-2164-11-206

36 Webster WS, Lohse CM, Thompson RH, Dong H, Frigola X, Dicks DL, Sengupta S, Frank I, Leibovich BC, Blute ML,

Cheville JC and Kwon ED: Mononuclear cell infiltration in clear-cell renal cell carcinoma independently predicts patient survival. Cancer *107(1)*: 46-53, 2006. PMID: 16708355. DOI: 10.1002/cncr.21951

37 Thompson RH, Dong H, Lohse CM, Leibovich BC, Blute ML, Cheville JC and Kwon ED: PD-1 is expressed by tumor-infiltrating immune cells and is associated with poor outcome for patients with renal cell carcinoma. Clin Cancer Res *13(6)*: 1757-1761, 2007. PMID: 17363529. DOI: 10.1158/1078-0432.CCR-06-2599

38 Attig S, Hennenlotter J, Pawelec G, Klein G, Koch SD, Pircher H, Feyerabend S, Wernet D, Stenzl A, Rammensee HG and Gouttefangeas C: Simultaneous infiltration of polyfunctional effector and suppressor T cells into renal cell carcinomas. Cancer Res *69(21)*: 8412-8419, 2009. PMID: 19843860. DOI: 10.1158/0008-5472.CAN-09-0852

39 Geissler K, Fornara P, Lautenschläger C, Holzhausen HJ, Seliger B and Riemann D: Immune signature of tumor infiltrating immune cells in renal cancer. Oncoimmunology *4(1)*: e985082, 2015. PMID: 25949868. DOI: 10.4161/2162402X.2014.985082

40 Hendry S, Salgado R, Gevaert T, Russell PA, John T, Thapa B, Christie M, van de Vijver K, Estrada MV, Gonzalez-Ericsson PI, Sanders M, Solomon B, Solinas C, Van den Eynden GGGM, Allory Y, Preusser M, Hainfellner J, Pruneri G, Vingiani A, Demaria S, Symmans F, Nuciforo P, Comerma L, Thompson EA, Lakhani S, Kim SR, Schnitt S, Colpaert C, Sotiriou C, Scherer SJ, Ignatiadis M, Badve S, Pierce RH, Viale G, Sirtaine N, Penault-Llorca F, Sugie T, Fineberg S, Paik S, Srinivasan A, Richardson A, Wang Y, Chmielik E, Brock J, Johnson DB, Balko J, Wienert S, Bossuyt V, Michiels S, Ternes N, Burchardi N, Luen SJ, Savas P, Klauschen F, Watson PH, Nelson BH, Criscitiello C, O'Toole S, Larsimont D, de Wind R, Curigliano G, André F, Lacroix-Triki M, van de Vijver M, Rojo F, Floris G, Bedri S, Sparano J, Rimm D, Nielsen T, Kos Z, Hewitt S, Singh B, Farshid G, Loibl S, Allison KH, Tung N, Adams S, Willard-Gallo K, Horlings HM, Gandhi L, Moreira A, Hirsch F, Dieci MV, Urbanowicz M, Brcic I, Korski K, Gaire F, Koeppen H, Lo A, Giltnane J, Rebelatto MC, Steele KE, Zha J, Emancipator K, Juco JW, Denkert C, Reis-Filho J, Loi S and Fox SB: Assessing tumor-infiltrating lymphocytes in solid tumors: a practical review for pathologists and proposal for a standardized method from the International Immuno-Oncology Biomarkers Working Group: Part 2: TILs in melanoma, gastrointestinal tract carcinomas, non-small cell lung carcinoma and mesothelioma, endometrial and ovarian carcinomas, squamous cell carcinoma of the head and neck, genitourinary carcinomas, and primary brain tumors. Adv Anat Pathol *24(6)*: 311-335, 2017. PMID: 28777143. DOI: 10.1097/PAP.0000000000000161

41 Rayman P, Wesa AK, Richmond AL, Das T, Biswas K, Raval G, Storkus WJ, Tannenbaum C, Novick A, Bukowski R and Finke J: Effect of renal cell carcinomas on the development of type 1 T-cell responses. Clin Cancer Res *10(18 Pt 2)*: 6360S-6366S, 2004. PMID: 15448031. DOI: 10.1158/1078-0432.CCR-050011

42 Fridman WH, Pagès F, Sautès-Fridman C and Galon J: The immune contexture in human tumours: impact on clinical outcome. Nat Rev Cancer *12(4)*: 298-306, 2012. PMID: 22419253. DOI: 10.1038/nrc3245

43 Hu J, Chen Z, Bao L, Zhou L, Hou Y, Liu L, Xiong M, Zhang Y, Wang B, Tao Z and Chen K: Single-cell transcriptome analysis reveals intratumoral heterogeneity in ccRCC, which results in different clinical outcomes. Mol Ther *28(7)*: 1658-1672, 2020. PMID: 32396851. DOI: 10.1016/j.ymthe.2020.04.023

44 Dai S, Zeng H, Liu Z, Jin K, Jiang W, Wang Z, Lin Z, Xiong Y, Wang J, Chang Y, Bai Q, Xia Y, Liu L, Zhu Y, Xu L, Qu Y, Guo J and Xu J: Intratumoral $CXCL13^{+}CD8^{+}$T cell infiltration determines poor clinical outcomes and immunoevasive contexture in patients with clear cell renal cell carcinoma. J Immunother Cancer *9(2)*: e001823, 2021. PMID: 33589528. DOI: 10.1136/jitc-2020-001823

45 Lin E, Liu X, Liu Y, Zhang Z, Xie L, Tian K, Liu J and Yu Y: Roles of the dynamic tumor immune microenvironment in the individualized treatment of advanced clear cell renal cell carcinoma. Front Immunol *12*: 653358, 2021. PMID: 33746989. DOI: 10.3389/fimmu.2021.653358

46 Vitale MG and Cartenì G: Clinical management of metastatic kidney cancer: the role of new molecular drugs. Future Oncol *12(1)*: 83-93, 2016. PMID: 26617188. DOI: 10.2217/fon.15.283

47 Motzer RJ, Tannir NM, McDermott DF, Arén Frontera O, Melichar B, Choueiri TK, Plimack ER, Barthélémy P, Porta C, George S, Powles T, Donskov F, Neiman V, Kollmannsberger CK, Salman P, Gurney H, Hawkins R, Ravaud A, Grimm MO, Bracarda S, Barrios CH, Tomita Y, Castellano D, Rini BI, Chen AC, Mekan S, McHenry MB, Wind-Rotolo M, Doan J, Sharma P, Hammers HJ, Escudier B and CheckMate 214 Investigators: Nivolumab plus ipilimumab *versus* sunitinib in advanced renal-cell carcinoma. N Engl J Med *378(14)*: 1277-1290, 2018. PMID: 29562145. DOI: 10.1056/NEJMoa1712126

48 Anker J, Miller J, Taylor N, Kyprianou N and Tsao CK: From bench to bedside: How the tumor microenvironment is impacting the future of immunotherapy for renal cell carcinoma. Cells *10(11)*: 3231, 2021. PMID: 34831452. DOI: 10.3390/cells10113231

49 Braun DA, Bakouny Z, Hirsch L, Flippot R, Van Allen EM, Wu CJ and Choueiri TK: Beyond conventional immune-checkpoint inhibition - novel immunotherapies for renal cell carcinoma. Nat Rev Clin Oncol *18(4)*: 199-214, 2021. PMID: 33437048. DOI: 10.1038/s41571-020-00455-z

Received January 12, 2022
Revised February 5, 2022
Accepted February 11, 2022